*metals*

MDPI

*Review*

# The Influence of Small Additions of Alloying Elements on the Hot Ductility of AHSS Steels: A Critical Review Part 2

**Barrie Mintz [1,*], Abdullah Qaban [1,*] and Shin Eon Kang [2,*]**

[1] Department of Mechanical Engineering and Aeronautics, University of London, London EC1V 0HB, UK
[2] Gwangyang Process Research Group, POSCO Technical Research Laboratory, POSCO, Pohang 37673, Republic of Korea
* Correspondence: barriejenny9@gmail.com (B.M.); abdullah.qaban@city.ac.uk (A.Q.); peterkang59@gmail.com (S.E.K.)

**Abstract:** In this paper, the influence of small additions of Cr, Mo, Cu, Ni, B, Ca, Zr, and Ce on the hot ductility of advanced high-strength steels (AHSS) has been reviewed. Most of these small additions have a positive effect in improving hot ductility on straightening during continuous casting operations and should be considered when problems with cracking in continuous casting are encountered. In many of these cases, the reason for these generally small but important improvements in hot ductility is not known with certainty, but the segregation of these elements to the austenite grain boundaries, strengthening the bonding, is often suggested.

**Keywords:** hot ductility; AHSS steels; Cr; Mo; Cu; Ni; Ca; Zr; Ce; B



**Citation:** Mintz, B.; Qaban, A.; Kang, S.E. The Influence of Small Additions of Alloying Elements on the Hot Ductility of AHSS Steels: A Critical Review Part 2. *Metals* **2023**, *13*, 406. https://doi.org/10.3390/met13020406

Academic Editor: Zhinan Yang

Received: 19 December 2022
Revised: 21 January 2023
Accepted: 27 January 2023
Published: 16 February 2023



## 1. Introduction

Advanced high-strength steels (AHSS), which include the TWIP (twinning-induced plasticity) and TRIP (transformation-induced plasticity) steels, have exceptional room-temperature ductility and strength. Both achieve these useful properties from having austenite present in their structure: TRIP steels have about 10% retained austenite in their microstructure, which can transform to martensite under deformation, thereby strengthening the steel; TWIP steels offer these properties via a totally different strengthening mechanism, that of twinning.

For TRIP steels, which undergo the austenite-to-martensite transformation, these properties are achieved by adding ferrite formers, Al, Si, and/or P, which delay the precipitation of pearlite, enabling carbide-free bainite to be formed with approx. 10% of high carbon-enriched retained austenite. These steels often have high Al (1–1.5 wt %), and/or Si (1–1.5 wt %) contents and may also contain high P contents (0.05 to 0.07% wt %) (all compositional percentages in the paper are shown as a weight percentage).The retained austenite, when under deformation, transforms to martensite, not only strengthening the steel but also improving its ductility by strengthening those regions that would otherwise thin down to failure. The TWIP steels, in contrast, are fully austenitic at room temperature and obtain their strength and good ductility from being able to twin under deformation. The large number of twins that are generated strengthen the steel, the twin boundaries behaving in much the same way as grain boundaries, in terms of preventing the free movement of dislocations. In order to achieve the required number of twins, the stacking fault energy (SFE) has to be controlled; if it is too high, this leads to cross-slip taking place, rather than twinning, while too low a SFE, leads to martensite formation. The composition is what mainly controls the SFE and again, in the TWIP steels, high levels of Al and Si additions are used, this time to adjust the steels' SFE to the necessary value.

Of the two types of strengthening mechanisms, greater strength and ductility can be achieved by twinning [1]. Due to their high room-temperature strength and formability, the automobile industry have taken a considerable interest in the development of AHSS steels

so that lighter weight vehicles can be produced by using thinner-gauge steel, so reducing the energy requirements for driving them.

However, these steels are often difficult to continuous cast without cracking when undergoing straightening operation and this has hindered their development. Because of this problem, the hot ductility of these steel in the temperature range 700–1000 °C, the range in which the unbending operation takes place has become very important and a MDPI Special Issue, entitled "Continuous casting and the hot ductility of AHSS steels" has been set up, which is devoted to this topic. The first part of this review, entitled "The Influence of Precipitation, High Levels of Al, Si, P, and a Small B Addition on the Hot Ductility of TWIP and TRIP-Assisted Steels" has been published in *Metals* (see Reference [1]) and this second part completes the review.

The first part of this review [1] deals with the hot ductility of the main constituents which are responsible for the good properties of these alloys, namely, Al, Si, and P for the TRIP steels and C, Mn, Al, and Si for the, TWIP steels. The use of the hot ductility curves for assessing the likelihood of cracking occurring is also thoroughly discussed there.

This second part of the review deals with the hot ductility of these steels on adding small additions of selected elements, which can, at times, make a substantial difference to whether these steels can be cast successfully. This second part also examines the hot ductility behavior after adding other elements of interest that are often present in these steels, Cr, Mo, Ni, and Cu, as well as highlighting the benefits small Ce, Ca and Zr additions may give in reducing the appearance of cracking when straightening these steels. The important role of small additions of B in improving hot ductility is also discussed in more detail.

## 2. Influence of Cr and Mo on Hot Ductility

### *2.1. Influence of Cr and Mo Additions on the Hot Ductility of TRIP Steels*

For TRIP steels, it is important to add small quantities of ferrite formers, which can delay carbide precipitation and allow approximately 10% stable high-carbon retained austenite to be formed in an essentially ferritic carbide-free bainite structure (before carbide precipitation takes place); both Cr and Mo being are ferrite formers. The TRIP steels can then undergo the austenite to martensite reaction upon deformation, so that the room temperature strength and ductility will be increased, with the martensite strengthening those regions that would otherwise neck down to failure. Al, Si, and P have been the most favored additions for achieving this micro-structure and have been discussed fully in the previous publication [1], which should be read in conjunction with this review.

As there are few papers on hot ductility that are devoted specifically to TRIP steels, the previous data available on high-strength low-alloy (HSLA) steels will also be discussed, since the high-temperature behavior of these steels is very similar [1].

Cr and Mo additions are used mainly in TRIP rather than TWIP steels; as already mentioned, they are ferrite-formers. Mo is an excellent element to add because it favors bainite and if the cooling rate is fast enough, it is possible to avoid its transformation to a ferrite/pearlite microstructure. They also contribute to increasing the hardenability, which is important for achieving adequate room-temperature strength, particularly for TRIP steels, which require low C contents so that they can be welded easily. Both elements can form carbides, making them less suitable than Al, Si, and P for delaying carbide precipitation in the ferrite.

For TRIP steels, it is necessary to ensure that the temperature at the start of the martensite transformation (Ms) is below room temperature so that a reasonable amount of austenite (10–20%) is retained at room temperature. This can be achieved by increasing the C content in the austenite or by having larger amounts of alloying elements, as can be seen from a commonly used empirical equation (Equation (1) to calculate the Ms [2].

$$\text{Ms } (^{\circ}\text{C}) = 539 - 423\%\text{C} - 30.4\%\text{Mn} - 17.7\%\text{Ni} - 12.1\%\text{Cr} - 7.5\%\text{Mo} \quad (1)$$

To achieve this in the original TRIP steels, the C contents were high, at ~0.4% C, but weldability was then a problem, due to the ease of forming martensite and the fact that high-C martensite is very brittle. For the automobile industry, it is considered that the carbon level should not exceed 0.2% in order to successfully spot weld [3]. However, higher alloying additions, as an alternative, are generally found to be too expensive [4]; but through a creative processing route, outlined in Reference [1], low C levels (0.02–0.2% C) and Mn levels of ~1.4% Mn with very limited specific alloying additions can be used [5]. In TRIP steels, it is important to prevent pearlite forming and ensure that ferritic bainite is formed; this means that the cooling rate required after intercritical annealing has to be fast, although not as fast as is needed to form martensite [6]. Mo is particularly good at decreasing the critical cooling rate for bainite formation and so has a marked effect in suppressing the pearlite transformation.

The importance of the various elements on the room-temperature tensile strength of TRIP steels can be gauged from a multiple linear regression equation, derived by Mesplont et al., to establish the tensile strength (TS) of ferritic bainite steels [7].

$$\text{TS (MPa)} = 288 + 803\%\text{C} + 83\%\text{Mn} + 178\%\text{Si} + 122\%\text{Cr} + 320\%\text{Mo} + 60\%\text{Cu} + 1180\%\text{Ti} + 1326\%\text{P} + 2500\%\text{Nb} + 36{,}000\%\text{B} \quad (2)$$

TRIP steels are softer than bainitic steels having ~10% austenite present as well as the hard ferritic bainite, but this equation (2) can also be applied to the TRIP steels if the constant is adjusted to a lower value [6]. Although, as shown in Equation (2), C can be very effective in increasing strength, both Cr and Mo can be used to lower the C content. According to this Equation (2) a reduction in C by 0.2% would require an addition of 0.5% Mo or an addition of 1.3% Cr to compensate for the resulting loss in strength. This fits in with the favored TRIP steel compositional range, which is up to 0.8–1.3% Cr [8] and 0.3–0.4% Mo [9] so that C levels are rarely higher than 0.3%.

Unfortunately, data are sparse on hot ductility behavior when adding small additions of Cr, although Liu et al. [10] have recently examined the hot ductility of Nb-containing steel at two Cr levels, namely, 0.12 and 0.45%. The base composition of the steels was 0.14% C, 1.4% Mn, and 0.03% Nb. Generally, changes in hot ductility were small in the temperature range of 650–850 °C. The addition of 0.12% Cr narrowed the trough and reduced its depth very slightly (see Figure 1), giving a reduction in area (RA) value that is a few percent higher, where $RA = (A_o - A_f)/A_o \times 100$ and $A_o$ and $A_f$ are the initial and final area, respectively. The further increase in Cr to 0.45% widened the trough, while the RA value at the base of the trough fell by approximately 10% in RA value, compared to that of the Cr-free steel. The finer austenite grain size in the 0.12% Cr steel probably accounted for its better ductility, although it is not clear what caused this refinement. Ductility at the base of the trough between 750 and 825 °C was poor, at <40% RA for the Cr-free steel and the 0.45% Cr steel, whereas for the finer-grained 0.12% Cr steel, the RA values at the relevant temperatures were generally > 40%, a commonly used value to give freedom from cracking [10].

The influence of Mo additions on hot ductility gives a clearer picture than with Cr, generally improving the ductility if enough Mo is added. Hannerz [11] found that Mo additions up to 0.3% had no influence on the hot ductility curve for a Nb-containing low C steel, but a higher addition of 0.6% lifted the bottom of the trough so that the RA value increased by ~5%, which, although small, may be important for the straightening operation (see Figure 2).

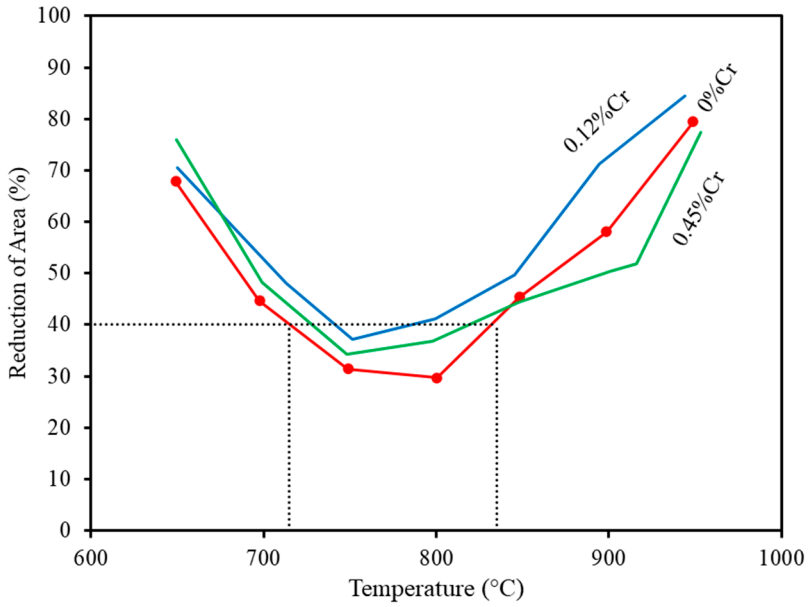


**Figure 1.** The hot ductility curves of an HSLA steel with base composition 0.14% C, 1.45% Mn, 0.029% Nb, and 0.002% N for three levels of Cr, 0, 0.12, and 0.45% [10], with permission from publisher Spring Nature, 2023.

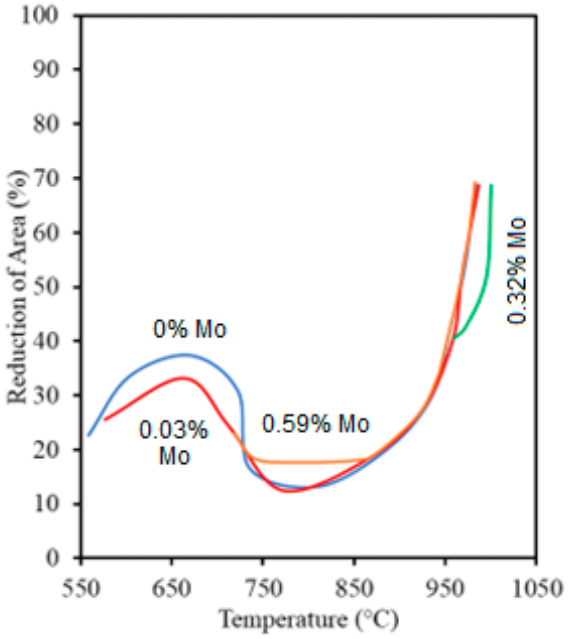


**Figure 2.** The influence of Mo on the hot ductility of Nb-containing HSLA steels. The steels had the composition of 0.07% C, 0.3% Si, 1.57% Mn, 0.008% P, 0.007% S, 0.037% Nb, 0.039% Al, and 0.015% N and contained nil, 0.03, 0.32, and 0.59% Mo shown as blue, red, brown and green curves, respectively [11].

Zheng et al. [12] have recently examined the influence of Nb (0.04%), V (0.06%), Mo (0–0.5%), and B (0.002%) on the hot ductility of a Cr–Mo medium C steel (0.27% C) with a low N (0.002%) level (see Figure 3). The addition of Nb and V both decreased the ductility, due to the fine precipitation of Nb(CN) and VN, respectively, with B again improving ductility. Two strain rates were used, one for the straightening operation, and the other for hot rolling. With this steel, the Ae3 temperature was low (~750 °C) so that the trough does not appear until just below 750 °C. For the part of the authors' investigation devoted to the influence of Mo on hot ductility, the base composition of the steel was 0.27% C, 0.72%

Mn, 1.1% Cr, 0.04% Nb, 0.002% B, and 0.0015% N. The addition of 0.25% Mo to this steel improved the ductility with a further increase to 0.5% giving an even greater improvement (Figure 3). Zheng et al. [12] suggest that this improvement is because molybdenum inhibits the formation of ferrite on cooling so that the ferrite film is removed (Figure 3).

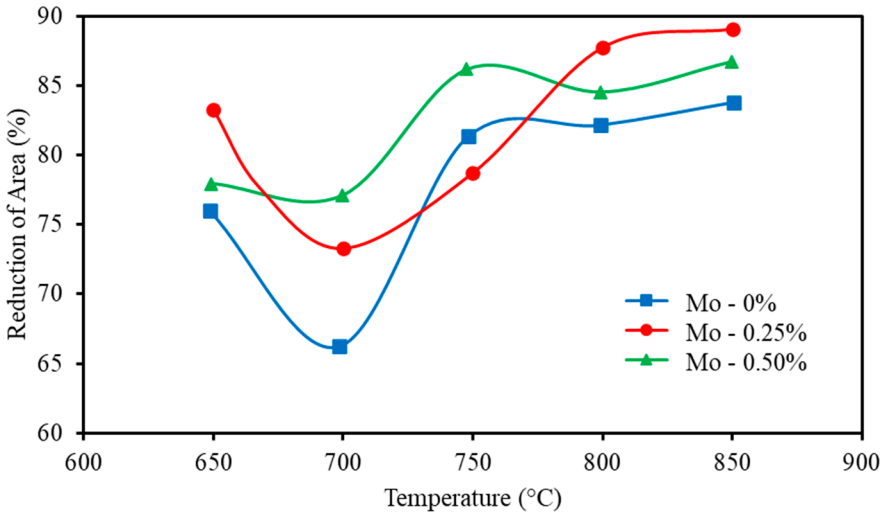


**Figure 3.** Influence of Mo on the hot ductility of an AHSS steel. The steels had a base composition of 0.27% C, 0.71% Mn, 1.1% Cr, 0.04% Nb, 0.12% V, 0.002% B, and 0.002% N, and contained 0%, 0.25% and 0.5% of Mo [12].

Although the hot ductility for higher amounts of Cr at ≥1% has not been explored, there is little evidence for any benefit in terms of hot ductility to be found in previous work, in that the RA values in the straightening temperature range are often reported at <40%, this being the RA value often taken below which cracking can occur [1]. This suggests that when these elements are present as major alloying additions, they are not, in themselves, beneficial to hot ductility, probably due to their tendency to form carbides.

### *2.2. Hot Ductility on Adding Cr and Mo to TWIP Steels*

Meija et al. [13] have added a Mo addition of 0.3% to a TWIP steel, the as-cast tensile specimens being taken from both sand-casting and metal molds, so as to give a variation in cooling rates as well as in the as-cast grain size. At a test temperature of 700 °C, the ductility for those samples cast in the metallic mold was similar for both the Mo-free and Mo-containing steels, both being ~40%. At an intermediate temperature of 900 °C, where dynamic recrystallisation (DRX) was detected in the Mo-containing steel, the ductility for the Mo-containing steel was significantly better (~70% RA) than in the Mo-free steel (~30% RA). The hot ductility curves are shown in Figure 4. Again, as with TRIP steels, there is no evidence that Mo, in itself, will cause any deterioration in ductility, and, indeed, can be beneficial.

However, the good ductility shown here in the temperature range of 800–950 °C (Figure 4) as a result of the Mo addition may not apply to the straightening operation, as the strains in the industrial straightening operation are too small for DRX to take place [1]. These high-Mn TWIP steels can then show worse ductility rather than better performance in the un-recrystallized state, the state present when straightening, as grain boundary sliding outpaces recovery at higher temperatures in the straightening temperature range [1].

Since much greater amounts of Cr are required to give a similar room-temperature strength benefit, Mo would seem to be the more suitable addition to increase the yield strength and maintain good ductility in the resulting TRIP steel. However, Mo can also form a carbide and so can have an adverse influence on hot ductility performance. Nevertheless, from the limited information available, solely from a hot ductility perspective, the addition

of Cr in excess of 0.15% would not be recommended, whereas the addition of Mo appears to have little influence at the lower levels and is beneficial at the 0.5% level.

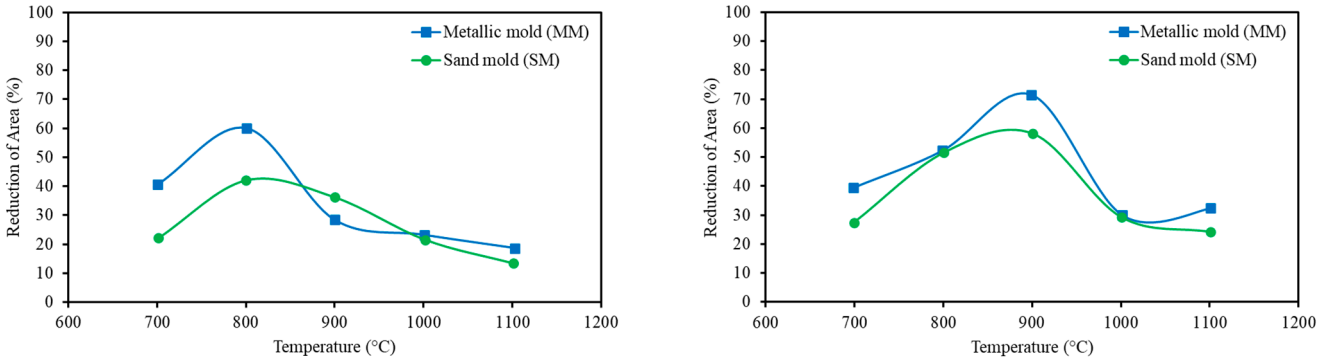


(**a**) Mo-free steel (**b**) 0.3% Mo

**Figure 4.** Hot ductility curves of the as-cast TWIP steel, having a base composition of 0.5% C, 21% Mn, 1.3% Si, 1.5% Al, and 0.012% N: (**a**) with no Mo present in the steel; (**b**) a 0.3% Mo addition. Tensile specimens were machined from sand molds or ingot castings, so as to give two cooling rates, a slow cooling rate with the sand molds and a fast cooling rate with the metallic molds. The 0.3% Mo addition can be seen to improve ductility in the intermediary temperature range of 800 to 950 °C, independent of the cooling conditions [13]. Adapted from [13], with permission from Elsevier, 2023.

## 3. Influence of Boron on Hot Ductility

### *3.1. Influence of B on the Hot Ductility of Ti-Free Low-C Steels, Including TRIP*

Boron is used in steels, principally to improve hardenability. For this, the benefit is only derived when in solution in the austenite [14,15]. Its solubility in both ferrite and austenite is very low; for example, in austenite at 900 °C, it is only ~0.003% [16]. However, even amounts as low as 0.0015% can substantially increase the hardenability. Boron has a great affinity for combining with N to form BN as well as carbon, to form $Fe_{23}(B,C)_6$ and $B_4C$; therefore, greater additions are often made to ensure that there is sufficient B in solution to allow segregation to the boundaries. When Ti is added to boron-treated steels, it preferentially combines with the N; and provided that there is sufficient Ti to exceed the stoichiometric composition for TiN, then the B addition can be limited to 0.003% [17].

Although B additions are mainly used to increase the hardenability of steels, B is now finding another important role in improving the hot ductility performance. Of all the microalloying additions, including Ti [18–20], Ca [21], Zr [18], Y [18], and Ce [22], which have been suggested for this purpose, B is probably the most cost-effective [14].

A boron addition is generally beneficial to the hot ductility of all steels, whether low- or high-C, often improving the ductility by a similar amount throughout the temperature range s covering the ductility trough (Figure 5) [23]. Its success applies equally to both TRIP and TWIP steels. Most importantly, as can be seen in Figure 5, it reduces the depth of the trough, which is believed to reflect the hot ductility of the un-recrystallized austenite [1,24] and so is relevant to the straightening operation. Lopez-Chipres et al. [23] suggest that the improvement in hot ductility behavior, shown in Figure 5 upon increasing the B content, is due to the segregation of boron to the austenite grain boundaries, increasing the resistance to grain-boundary sliding.

However, a multitude of reasons have been given for this improvement and it is unlikely that there is only one reason for its beneficial effect on hot ductility. The grain boundary segregation of B strengthen e the austenite grain boundaries; therefore, discouraging grain boundary sliding seems always to be important [23,25]. Boron encouraging the formation of DRX by segregating to the boundaries and decreasing the mobility of grain boundary dislocations has also been suggested [26]. Another explanation is that boron is able to diffuse so rapidly, it being such a small atom, that it is able to keep pace with the moving boundary during hot deformation, creating a drag on its movement and thereby

refining the dynamically recrystallized austenite grain size and enhancing ductility [27–29]. The ductility, therefore, improves as the boron level increases.

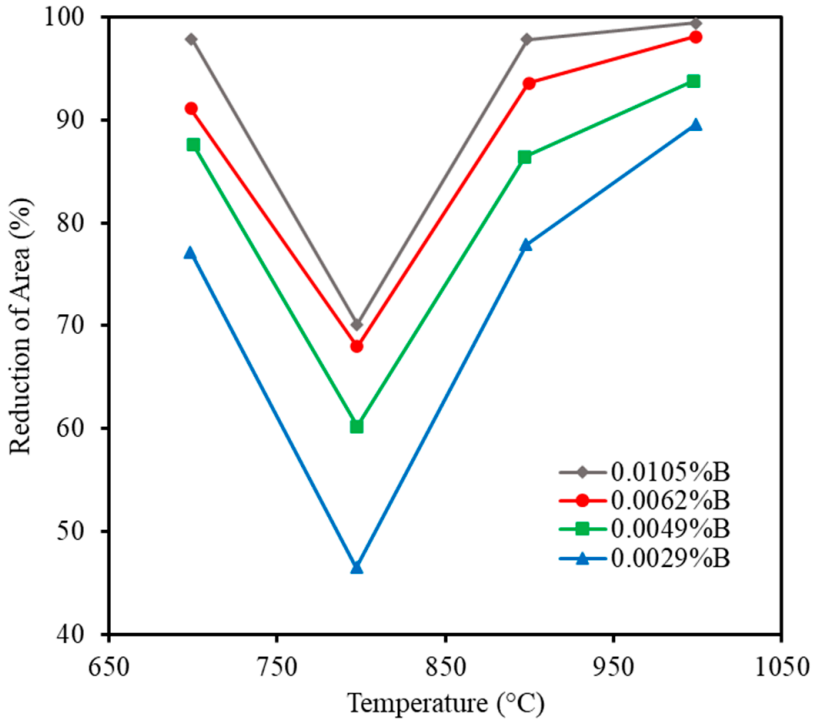


**Figure 5.** Hot ductility curves for a series of plain C-Mn steels with varying amounts of boron, from 0.0029 to 0.0105%. Increasing the B level causes the ductility to improve. The steels had the following base composition of 0.04% C, 1.6% Mn, 0.025% Al, and 0.0085% N; they were solution-treated at 1100 °C, held there for 5 min, and were then strained to failure at a strain rate of $10^{-3}$·$s^{-1}$ [23]. Adapted from [23], with permission from Elsevier, 2023.

Yet another reason that has been given is that when B precipitates out in the matrix, it encourages the nucleation of ferrite there, rather than at the boundaries as a thin film [30]. This is illustrated very convincingly in Kim et al.'s work (see Figure 6) [30]. They suggest that the coarse $Fe_{23}(B,C)_6$ particles that are present within the prior austenite grains act as preferential sites for the intragranular nucleation of ferrite. Kim et al. [30] also suggest that, in addition to the more homogeneous distribution of ferrite preventing strain concentration, thereby avoiding low ductility and ductile intergranular failure, a B addition might also lead to refinement of the recrystallized austenite grain size [30]. The addition of 0.002% boron that Kim et al. made to a 0.08% C, 1.0% Mn, 0.02% Nb, 0.005% N, and 0.025% Al, low S (0.003%)-containing steel completely removed the ductility trough, giving RA values of >90%. Ductility was good, even without the addition of boron; the minimum RA was 53% at 750 °C, but the addition of boron yielded, on average, a 30% improvement in the RA values throughout the testing temperature range of 700–850 °C (see Figure 6c) [30].

Similar but less impressive improvements were noted by Song et al. [31] for a Cr- and Mo-alloy steel; again, they point out that B not only reduces the width of the hot ductility trough but also decreases the depth of the trough (see Figure 7).

Campbell [32,33] also considered boron to be a beneficial element in preventing transverse cracking during casting, through the inhibition of bi-film formation; the boron addition reduced the melting temperature of the surface oxide in the liquid steel. The borates (boron oxides) that formed on the surface of the liquid steel would have a melting point as low as 1000 °C [32].

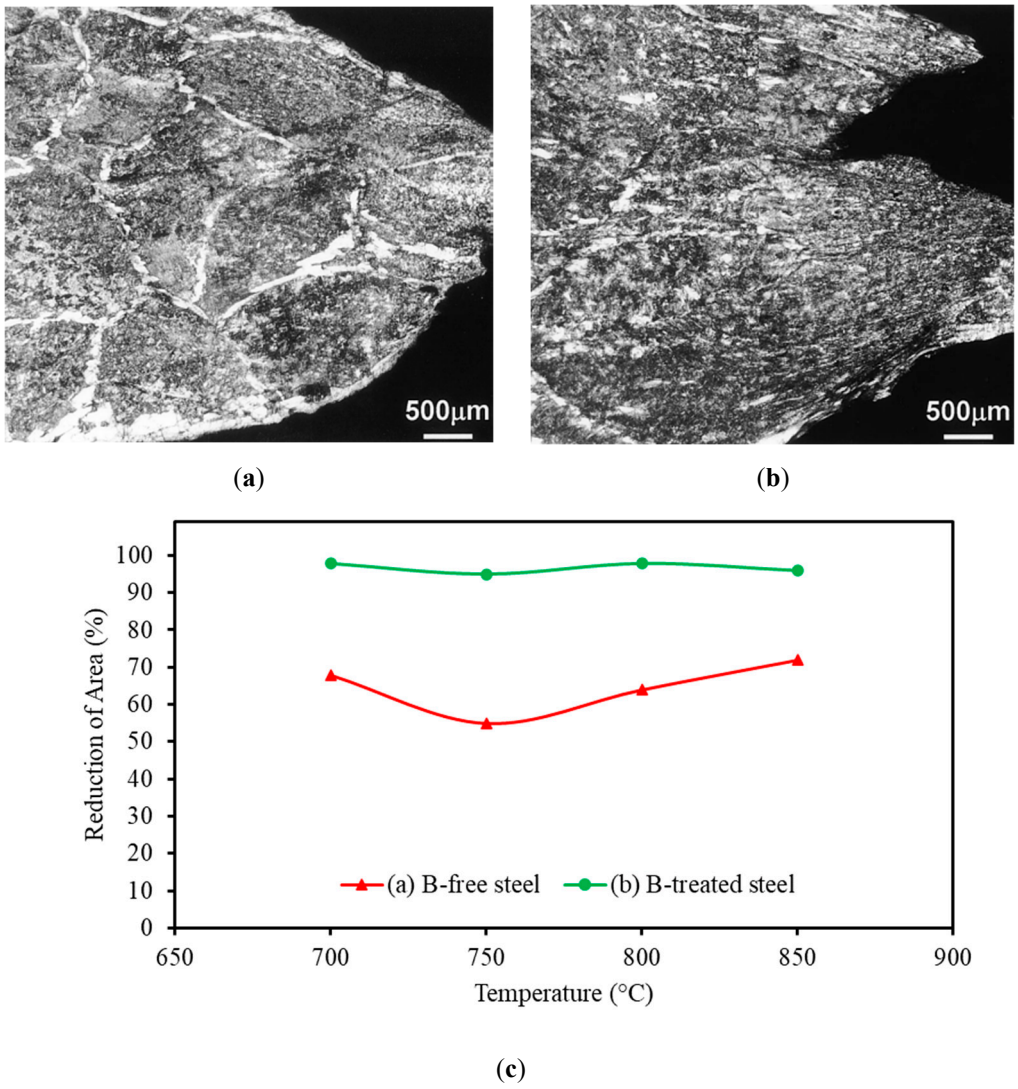


**Figure 6.** The change in ferrite distribution from the boundaries to the matrix by adding 0.002% B, in samples tested at 750 °C. (**a**) No B, ferrite at boundaries; (**b**) with 0.002% B addition, ferrite was distributed at the boundaries and within the matrix; (**c**) hot ductility curves for the two steels [30]. Adapted from [30], with permission from Elsevier, 2023.

Another advantage of boron is that the detrimental effect of both P and S on hot ductility can be prevented by the addition of boron, which segregates to the boundaries much faster than would occur with these elements, both in ferrite and austenite and once there, the boron strengthens rather than weakens them [31,34,35]. In the case of P [31] and S [35], the interfacial energy of the grain boundary (cohesive strength) is lowered, whereas, in contrast, it is believed that B strengthens the bonding at the boundaries [25]. B diffuses much faster than these other elements and, in any competition, will always arrive at the vacant sites first. Hence, B can occupy sites that would otherwise be occupied by P [34]. This may also explain the benefit in terms of ductility from adding B to the high P-containing TRIP steel in Figure 8 [36]; however, this steel also had Ti as a microalloying addition, so the benefit is just as likely, in this instance, to be due to B occupying the vacant sites needed for the fine deleterious precipitation of TiN. This is similar to the way in which P, in the absence of B, can, on occasion, be beneficial to hot ductility behavior by occupying the vacant sites for the more deleterious fine dynamic precipitation of Nb(CN) [37].

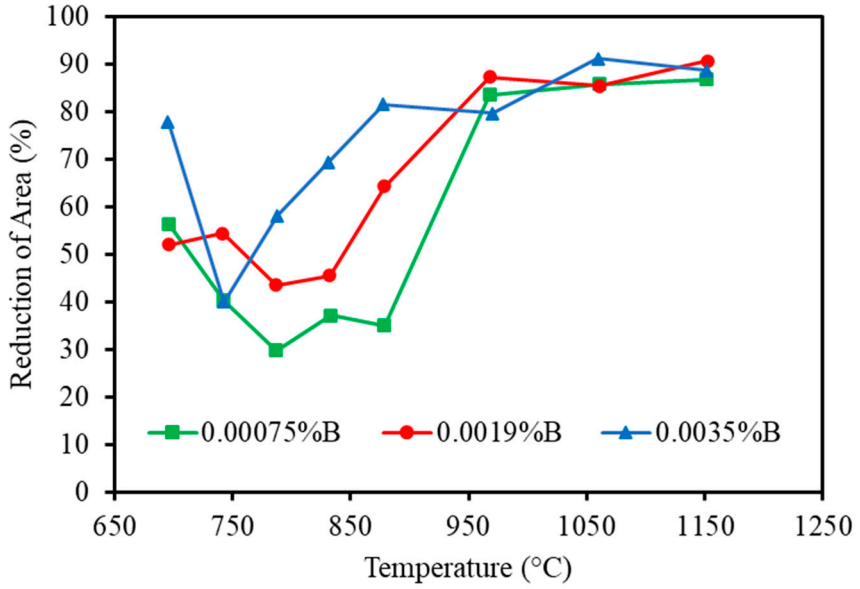


**Figure 7.** Hot ductility curves for specimens doped with different quantities of boron. The base composition of steel was 0.12% C, 0.25% Si, 0.5% Mn, 0.15% Al, 2.3% Cr, and 0.95% Mo [31]. Adapted from [31], with permission from Elsevier, 2023.

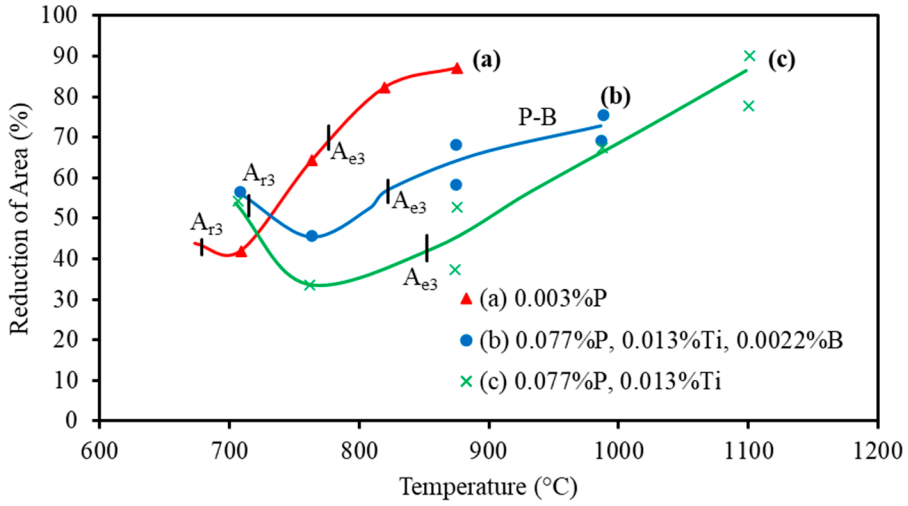


**Figure 8.** Hot ductility curves for C-Mn TRIP-assisted steels (0.15–0.2% C, 1–1.45% Mn, 0.3% Si): (curve a) 0.003% P; (curve b) 0.077% P, 0.013% Ti and 0.0022% B; (curve c) 0.077% P and 0.013% Ti [36]. Adapted from [36], with permission from Taylor & Francis Group, 2022.

Recently, to add to the list, it has been found that B refines the as-cast grain size in high Mn and high Al TWIP steels [38,39], which would increase the fracture strength, this being particularly important for improving the ductility in the straightening operation where DRX is not possible.

It has also been shown [23,38,40,41] that B encourages dynamic recrystallization, as well as refining the grain size, probably, in the latter case, by slowing down the movement of the boundaries via solute drag [38]. The multitude of explanations to account for boron's beneficial effect is somewhat confusing, but these cannot detract from its generally beneficial effect on hot ductility.

Strain rates are so slow during the straightening operation (~0.001 $s^{-1}$ for thick slab casting) that the information given by creep experiments can be very helpful in understanding the role of B in improving ductility. Nix et al. [42] have shown with physical models

how the segregation of atoms to the boundaries can influence the speed of intergranular crack growth under creep conditions. Earlier works by Lagerquist and Lagneborg [25] also showed that the detrimental effect of grain-boundary sliding upon fracture is minimized by B-segregation, thereby enabling creep ductility improvement. This is one of the reasons that Hannerz [11] has given for the marked improvement in hot ductility that he found upon adding B, as shown in both the simple hot ductility test and from the commercial statistics on the slab-cracking susceptibility when straightening.

A more recent study by Laha et al. [43] suggested that the improvement in creep ductility shown by B-bearing steels was due to B taking up vacant sites at the austenite grain boundaries and hindering the formation of micro-cavities, thereby significantly decreasing their growth rate. The study was carried out on an austenitic stainless steel in which both B (0.069%) and Ce (0.016%) were added to the steel. Both elements were found to segregate to the surface of the expanding cavities at the boundaries, suggesting that the removal of S, at which Ce is very effective, and the presence of B at the boundaries were preventing these vacancies from being available for the growth of micro-cavities.

However, it is important to note that B is also capable of causing the hot ductility performance to deteriorate. Boron has a high affinity with N, forming a nitride, which, when fine, is detrimental to ductility. When casting these steels, care has to be taken to ensure that the B is there in solution in the austenite or, at least, when precipitated as BN, in an un-harmful coarse form. BN precipitates can encourage intergranular fracture, as shown by Yamamoto et al. [44], Cho et al. [45], Wang et al. [46], and Taguchi et al. [47]; the finer they are, the worse the ductility. Cho et al. [45] found that increasing the cooling rate from 60 to 1200 °C/min (1 °C /s to 20 °C /s) in a low C, Mo, and Al killed steel (0.025% Al) had no influence on the hot ductility (see Figure 9a); however, when B was added (see Figure 9b), the ductility improved at the slowest cooling rate of 60 °C/min, by ~10% RA, but then became progressively worse as the cooling rate increased, the depth and width of the trough increasing as the BN precipitation became finer. This bar the initial improvement in ductility is a similar behavior to that observed with other microalloying precipitates containing V, Nb, and Ti in HSLA steels, the ductility deteriorating with increase in cooling rate and consequent refinement of the precipitates [37]. The cooling rate is very important for the segregation of B to the boundaries, this segregation being both equilibrium and non-equilibrium [29,48–51], so that the back diffusion of B from the boundary to the matrix can make a large difference to the final ductility. If the cooling rate is outside a certain range of 10–100 °C/min, segregation will be very much reduced (see Figure 9a) [52]. Taguchi et al. [47] have also suggested that adding 0.011% Zr can prevent B from precipitating out at the austenite grain boundaries in a steel with 0.1% C, 1.4% Mn, 0.01% Ti, 0.0017% B, and 0.005% N, as B finds the oxide of Zr in the matrix to be a favored site for the nucleation of BN, rather than at the boundaries, thereby making DRX easier. As with Ti, Zr is a very powerful nitride former and, as long as the nitride-forming precipitates are away from the boundaries, they can prevent BN from forming there and can allow the unimpeded segregation of the remaining B to the boundaries.

Cho et al. [45] and Shen et al. [53] also highlight that the detrimental influence of BN on the hot ductility of Ti-free steels of a composition given in Figure 9 can be alleviated, and corner cracks avoided, by keeping the N as low as possible and slowing down the cooling rate after solidification, whenever possible [45]. With high cooling rates in the lower austenite temperature range, the BN precipitates preferentially at the austenite grain boundaries as a fine precipitate, favoring intergranular failure. At slower cooling rates, the precipitation of BN was found to be random, coarser, and sparse [45].

Cho et al. [45] and Laha et al. [43] suggest that when B is present as a solute atom at the boundaries, it occupies vacant sites that were formed upon deformation and so prevents cracks formed by the grain boundary sliding (GBS) from joining up. However, when B forms a nitride, it pins the boundaries and allows cracks to join up by void formation. Hence, the surface defects and cracks that have formed on continuously cast billets have often been attributed to BN precipitation in boron-bearing steels [45,54,55].

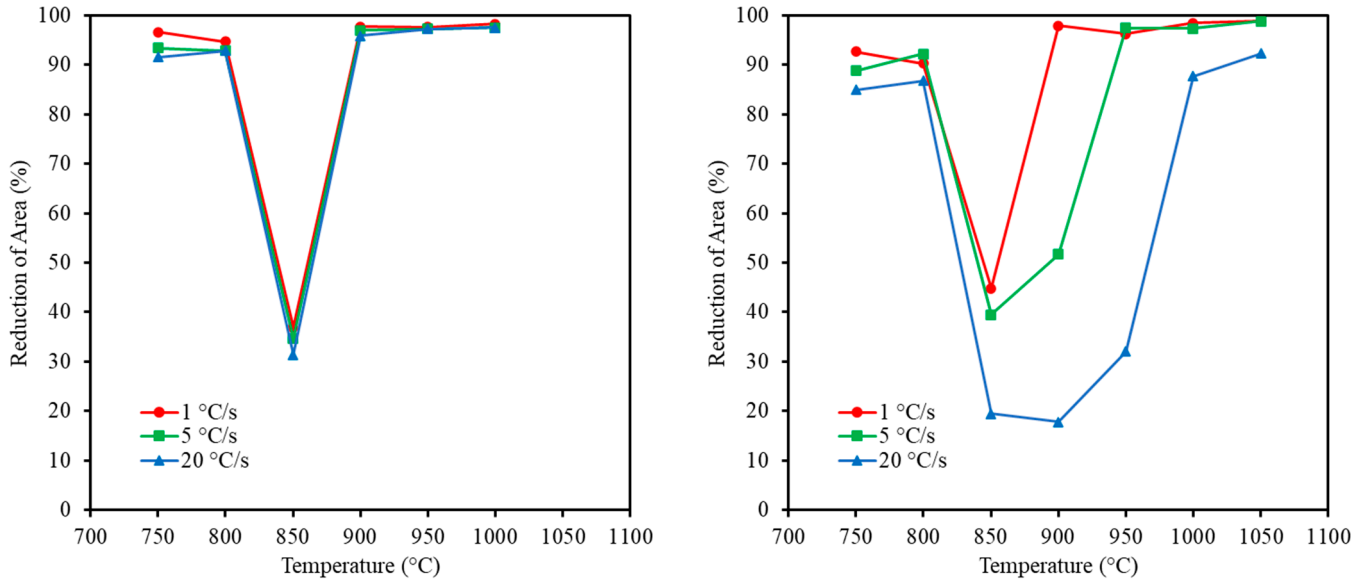


**Figure 9.** Hot ductility curves at various cooling rates for: (**a**) B-free steel and (**b**) B-containing steel [45]. Adapted from [31], with permission from Springer, 2023.

### *3.2. Influence of the B/N Ratio on the Hot Ductility of Steels without Ti*

Nevertheless, as long as BN forms a coarse precipitate, it can also be used, as with Ti, to remove N from a solution and thereby prevent or reduce the amount of AlN forming at the boundaries, since AlN is so detrimental to ductility in low-Al and low-C steels [55].

Chown and Cornish [55] examined the hot ductility of a low N (~0.005%), Al-killed (0.04–0.055 Al%), low C-Mn steel at three levels of B, 0.001, 0.002, and 0.003%. Two strain rates, 0.001 $s^{-1}$ and 0.0001 $s^{-1}$, and three cooling rates of 18, 75, and 180 °C/min were included in the study, so as to cover both thick and thin slab continuous casting conditions. For the lowest B level (0.001%), the ductility was always poor at the test temperature of 900 °C (20–30%RA), independent of the condition, and only improved at higher temperatures when DRX took place. Ductility improved as the B level increased, and, at the highest level (~0.003%B), the hot ductility trough was completely eliminated, the B:N ratio then being 0.75, which is almost the stoichiometric ratio for BN (0.8:1). The RA values were then in excess of 80% for the test temperature range of 800–1050 °C. On the basis of these results, the slower cooling rate range was recommended (18–72 °C/min), as typically experienced in thick slabs and blooms; a low B:N ratio of 0.47 was adequate to avoid a ductility trough. However, at the high cooling rate of 180 °C/min that is associated with thin slab and billet casting, to avoid the trough, a higher B:N ratio of 0.75 was required [55]. The improvement in ductility was ascribed to B removing all the N as BN, rather than allowing the N to precipitate out more detrimentally as AlN at the austenite grain boundaries. The same study [55] again illustrates how damaging AlN can be to ductility. BN precipitation was also rendered innocuous as it co-precipitated on the sulfide inclusions, forming coarse complex precipitates that were too coarse to influence the hot ductility, the B having been shown to preferentially segregate to the MnS inclusions rather than the boundaries [56].

This explanation given by Song et al. [31] for the improvement of ductility by B addition is very different from that given by Lopez-Chipres et al. [23]. While working with plain C-Mn steel, they suggested that the segregation of B to the boundaries is responsible for better ductility [23]. The difference probably arises because, whereas the B range was very high in the work of Lopez-Chipres (0.003–0.01% B), the B range covered by Song et al. [31] did not exceed 0.003% (the range covered was 0.001–0.003% B). This meant that in the former case [23], shown in Figure 5, there was always enough B present in the solution to

be able to segregate to the boundaries. The B was engaged, first in mopping up all the N to form BN, thereby reducing the amount of AlN, which is more detrimental to ductility, and when the B level reached 0.003%, the remaining excess B in solution was free to segregate to the boundaries. This is also shown in Figure 7 [31] for a low-alloy steel, when the shape of the curve changes at the 0.0035%B level to the very narrow trough behavior shown in Figure 5. Only when the level of B reached the top of its range, at 0.003%, did segregation "kick in" [31]. In contrast, in the work of Lopez-Chipres, the B level was so high that B was always able to segregate unimpeded to the boundaries. This illustrates the difficulty in interpretation with there being so many different explanations for results, depending on the particular conditions examined. Again, B has been shown to encourage DRX [38,40], but Lis et al. [57] have also reported that if boron nitride forms, it can suppress the dynamic recrystallization of austenite during hot working. Indeed, the stress concentration created by these precipitates can weaken the grain boundary, encouraging grain boundary sliding, and so enhance the development of cracks, thereby reducing the elongation to fracture [57].

Importantly, for the present review, Meija et al. [58] found that the addition of 0.012%B to a low-C, low-alloy, Ti-free, TRIP-assisted AHSS steel enhanced the hot ductility performance significantly throughout the temperature range (650–1150 °C), as shown in Figure 10.

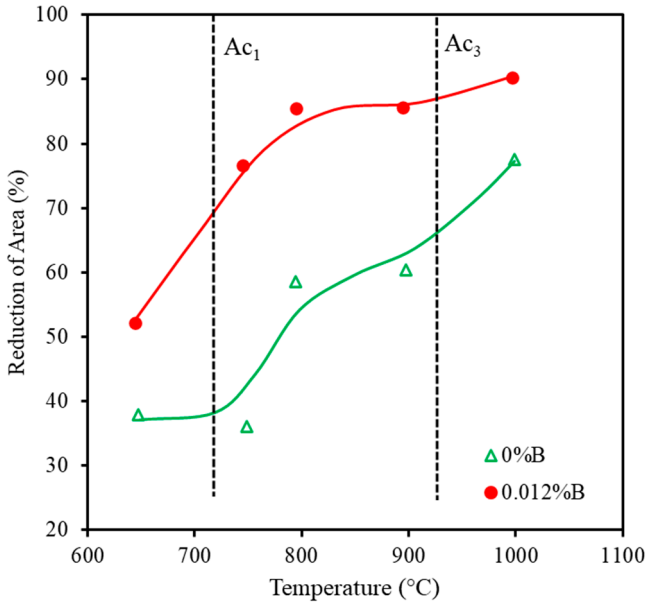


**Figure 10.** Influence of the addition of B (0.012%) on the hot ductility curve of low-carbon advanced high-strength steels (AHSS). The base composition of the steel was 0.06% C, 0.35% Mn, 0.3% Si, 2.2% Ni, 1.2% Cr, 0.5% Cu, 0.2% V, and 0.006% N, and was Ti-free [58]. Adapted from [58], with permission from Elsevier, 2023.

In this case, the tensile specimens were cast in situ and the tensile specimens were heated up to the test temperature, rather than being cooled down from the austenite. The poor ductility at low temperatures <850 °C was associated with the presence of inclusions and precipitates, particularly MnS and V(CN), which caused void formation on deformation, thereby enabling the cracks to propagate. The good ductility performance at the high end of the trough was due to DRX, as is normally the case (Figure 10). Again, the improvement in ductility upon adding B was of similar magnitude, independent of the test temperature, and clearly took place in the ferrite two-phase region and austenite. This is one of the main advantages of B, in that it can improve the ductility throughout the entire trough, the ductility at the base of the trough being relevant to the straightening operation and the better ductility at the high-temperature end of the trough, where DRX occurs, being relevant to hot forming operations.

### *3.3. Influence of Ti Additions on the Hot Ductility of Boron-Containing Low-Al Steels*

When the segregation of B to the boundaries is the main cause of an improvement in hot ductility, the maximum benefit occurs when B can segregate unimpeded to the boundaries and strengthen them. B is a strong nitride-forming element and, unless there is a stronger nitride-forming element present, such as Ti, if we are not careful, as has been already noted, BN often forms as a fine precipitation that is detrimental to ductility [55]. However, of the two precipitates, AlN is worse, as it precipitates preferentially at the austenite grain boundaries. Wang et al. [46] examined the precipitation of BN, AlN, and TiN via thermodynamic analysis and came to the conclusion that higher B contents led to fewer AlN precipitates, while the addition of Ti reduced the number of BN particles during solidification. This analysis can be applied to low-Al steels. Although AlN is, in fact, more stable than BN because of boron's smaller atomic size, it diffuses faster to form BN at the expense of AlN [59]. Other compounds, such as $Fe_{23}(B,C)_6$ and $B_4C$, can also form but they are coarser and less detrimental to hot ductility in comparison with boron–nitride compounds [31,39–41]. Therefore, for B to gain its full potential in improving hot ductility by strengthening the boundaries, very strong nitride-forming elements are required, such as Ti or Zr. Ti additions allow most of the N to combine with Ti to form one of the most thermodynamically stable nitrides. B can then segregate solely to the boundaries and so improve hot ductility, as observed in many studies [11,30,31,38,40,55,58].

Hannerz [11] found that even small B additions (0.002%) to steel (a B:N ratio of 0.18), can improve the ductility of low-C steels wherein Ti and Al are present (the base composition of the steel was 0.07% C, 1.5% Mn, 0.027% Al, 0.02% Ti, and 0.011% N) and, as with the findings of most other investigations, the improvement occurred throughout the temperature range of 800–1000 °C.

The TiN particles must also be coarse so as not to influence ductility, meaning that the cooling rate is always of critical importance.

### *3.4. Importance of Cooling Rate in Both Ti-Free and Ti-Containing Low C and Low Mn Steels*

As well as choosing the best composition to enhance ductility in B-containing steels, the cooling rate on cooling to the test temperature must be suitable. Yamamoto et al. [44] have examined the influence of cooling rate on the hot ductility of B-treated steels and have produced a map showing when ductility is satisfactory and when it is not (see Figure 11). It should be noted that a very high RA value of 60% was used as the criterion for good ductility. The authors of [44] show that for low-Al steels (<0.04% Al), there is a shaded area on the graph in Figure 11a, giving poorer ductility in which BN can form. This area can be seen to yield worse ductility in relation to those areas where BN was absent (Figure 11a,b).

An analysis of the various research papers examining cooling rates and the segregation of boron has concluded that cooling rates of between 10 and 100 °C/min favor boron segregation and lead to better ductility, the slower cooling rates being preferred for maximum segregation and coarsening of the precipitates [52]. Although slower cooling rates generally improve hot ductility by coarsening the particles, because segregation is a non-equilibrium state, there is an optimum "minimum" cooling rate. Coarser precipitates reduce the stress acting on the boundaries, making grain boundary sliding more difficult, and, when situated at the boundaries for a given volume fraction of precipitates, they make it more difficult for cracks to join up along the boundaries [37,39,52]. Yamamoto et al. [44] reported that the optimum cooling rate for the maximum segregation of B at grain boundaries was ~10 °C/min and that reducing the cooling rate from 1200 to 6 °C/min moved the BN precipitation from the austenite grain boundaries to the area within the grain interiors, where it had little influence on the ductility (Figure 11). TiN precipitation can also be very damaging for hot ductility but, again, if the cooling rate is ~10 °C/min, the TiN will have coarsened and will no longer influence the hot ductility behavior [60,61]. When there is no Ti present in the steel, the use of fast cooling rates induces fine BN precipitation in the matrix and at the grain boundaries. As well as preventing dynamic recrystallization by pinning grain boundaries or individual dislocations, this increases the shear stress acting

on the boundaries, encouraging grain-boundary sliding [44]. The fine precipitation at the boundaries results in short inter-particle spacing, allowing cracks to interlink more easily, and promoting intergranular failure due to microvoid coalescence.

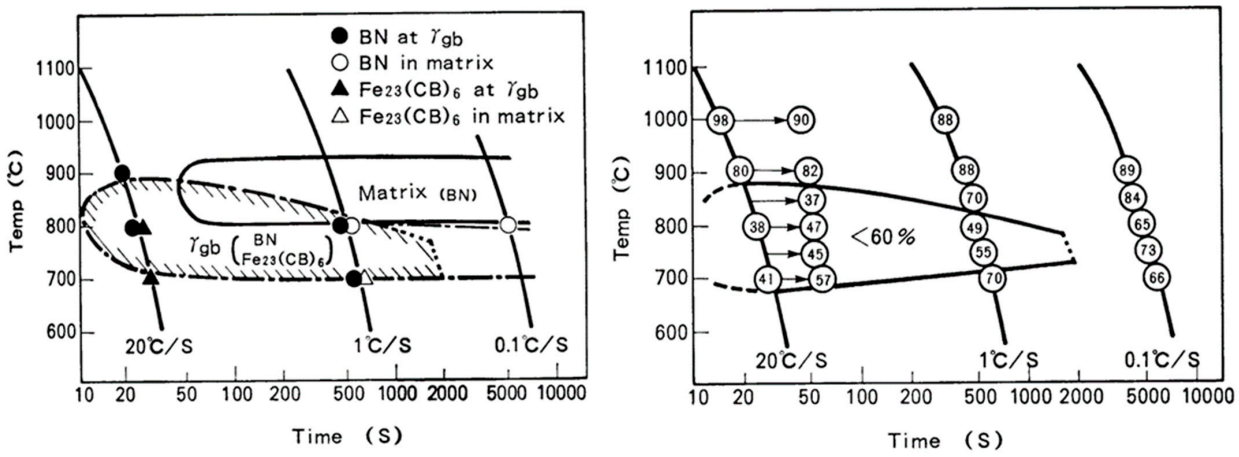


(**a**) (**b**)

**Figure 11.** (**a**) PTT (precipitation–temperature–time) diagram for BN precipitation, both in the matrix and at grain boundaries. (**b**) Temperature–time–ductility diagram for boron-treated steels, with the cooling rate curves for 3 different cooling rates, 20 °C/s, 1 °C/s, and 0.1 °C/s. The temperature range that yields lower ductility widens as the cooling rate increases, ductility occurring for all test temperatures at 0.1 °C/s with > 60%RA, decreases to 50%RA between 700 °C to 800 °C for the cooling rate of 1 °C/s, decreases further to 40%RA for the highest cooling rate 20 °C/s, and spans the widest temperature range of 670 °C to 870 °C. The numbers in circles are the RA values [44].

Zarandi and Yue [40] have found that, even with Nb-containing steels, small additions of boron at 0.002 and 0.004%, Nb-B1 and Nb-B2, respectively (Figure 12), are very beneficial to hot ductility, improving the ductility throughout the straightening temperature range of 700–1000 °C (see Figure 12). In contrast, the ductility of the boron-free Nb-containing steel (the green curve in the figure) was very poor. Fracture examination by Zarandi and Yue [40] indicated that in these Nb-containing steels, the failure mode in the trough was intergranular by GBS for the boron-free steel, whereas it was transgranular for the boron-containing steels.

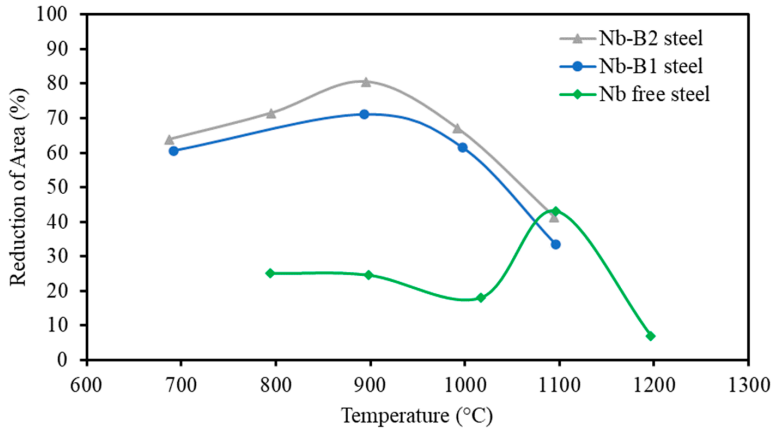


**Figure 12.** Hot ductility curves for Nb boron-containing steels and a Nb-boron-free steel. The Nb-boron-containing steels had the base composition of 0.015% C, 1.65% Mn, 0.05% Nb, 0.02% Ti, 0.005% N, and 0.008% S, and the B additions were 0.002% for B1 and 0.004% for B2. The boron-free, Nb-containing steel had a somewhat different composition, with 0.05% C and 0.009%N. A thermal schedule was used, which included undercooling [40].

The poor ductility of the Nb-containing, boron-free steel in Figure 12 may be because the Ti level was too low to combine with all the N (0.009%), together with a higher carbon level.

Yamamato et al. [44] have shown that the effectiveness of B in improving the hot ductility of steel depends mainly on the amount of Ti and N needed to ensure that all the N is bound to the Ti (usually in excess of stoichiometry), but the cooling rate needs to be chosen to give the maximum segregation of B to the boundaries, as well as to coarsen the TiN precipitates, i.e., ~10 °C/min.

## 4. Importance of Stacking Fault Energy (SFE) in Controlling the Composition of AHSS Steels

The composition of these steels very much influences the SFE, and this, in turn, influences the hot ductility performance. Although the SFE is more relevant to the high Al- and Si-containing TWIP steels, the importance of SFE cannot be more heavily stressed for all these steels, as it controls whether a steel will have TRIP or TWIP characteristics and plays an important role in whether DRX occurs or not, thereby influencing the hot ductility performance. Deformation twins are formed upon shearing by the separation of two partial dislocations and the SFE energy is measured by the degree of separation; the narrower the spacing between these partial dislocations, the higher the SFE. Transmission electron microscopy (TEM) can be used to measure this width and thereby calculate the strength of the SFE [62]. If the energy is high, the partial dislocations only separate by a small distance and cross-slip is favored rather than twinning. On lowering the SFE, a stage is reached in which cross-slip is difficult and twinning is favored. If the energy is too low, cross-slip becomes no longer possible, resulting in a considerable increase in the dislocation density and consequent work-hardening, causing the austenite to transform to martensite rather than to twin. Hence, twinning only occurs over a narrow SFE range of 20–40 mJ $m^{-2}$ [63,64]. If the SFE is <20 mJ $m^{-2}$, work-hardening is excessive, and ε martensite forms [65,66], while if >40 mJ $m^{-2}$, normal glide takes place [63].

The thermodynamic calculations for the SFE have now reached the stage of offering reasonably good agreement with the measured experimental values, as can be seen from Figure 13, and it is, therefore, possible to use them to help design steels with the appropriate stacking fault energy. There are many equations and models that have been established and the more recent ones seem to be very satisfactory [64,66–71].

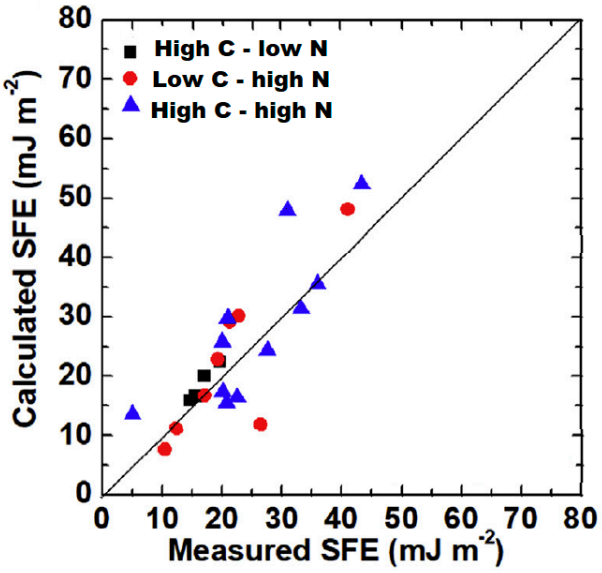


**Figure 13.** Relationship between thermodynamically-calculated SFE and experimentally measured SFE in Fe-Cr-Mn-C-N steels using most suitable thermodynamic parameters (see ref for thermodynamic parameters) [67].

However, before choosing a composition, as well as when satisfying the SFE requirement to facilitate twinning, it is also necessary for the austenite to be stable at room temperature. This means that for the current TWIP steels, a high Mn content is chosen (15–30%), to stabilize the austenitic structure at room temperature [63]. The two elements with the greatest influence in lowering the martensite start temperature (Ms) are C and Mn and a useful empirical relationship to obtain a fully austenitic structure at room temperature in the TWIP steels is quoted as:

$$\%\text{Mn} + 13\%\ \text{C} \geq 17. \quad (3)$$

This equation applies to steels with Mn contents of 15–30% and carbon contents of 0.1–0.8%. [63]. This means that even with a low C level, it is still possible to obtain fully austenitic steels at room temperature with a high Mn level; however, because decreasing the C content lowers the SFE, the TWIP requirement may not be met.

According to the thermodynamic calculations for Fe-Mn-high-C alloys with Mn contents of between 0 and 29%, the SFE decreases with increasing Mn concentration, up to approximately 13 wt %, and then rises again (see Figure 14a) [64].

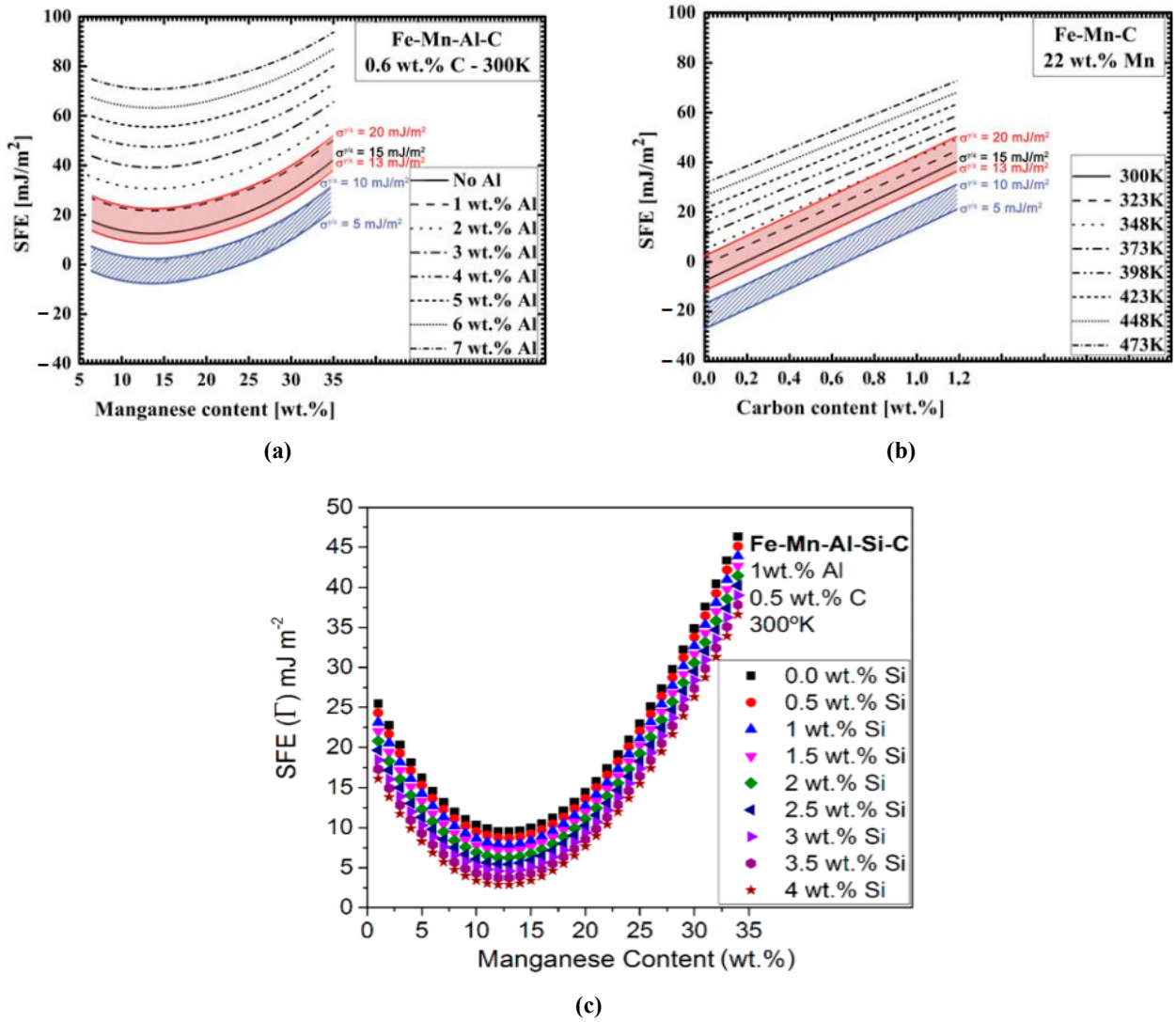


**Figure 14.** Composition-dependent SFE maps. (**a**) The influence of Mn and Al contents on SFE in a steel with 0.6% C [71]. Adapted from [71], with permission from Springer, 2023. (**b**) The influence of C content on the SFE in a steel with 22% Mn [71]. (**c**) The influence of Mn and Si on the SFE in a 0.5% C steel with 1% Al [64]. Adapted from [64], with permission from ASME Publications, 2023.

The experimentally measured SFEs for some of the TWIP steels in the study are given in Table 1 and vary between 15 and 41 mJ $m^{-2}$.

**Table 1.** Experimentally determined SFEs for some of the TWIP steels.

| TWIP Steel | Stacking Fault Energy mJ $m^{-2}$ | Ref. |
|---|---|---|
| Fe-18% Mn-1.5Al-0.6C | 30 | [64] |
| Fe-22% Mn-3Al-3Si -0.01C | 15 ± 3 | [68] |
| Fe-25% Mn-3Al-3Si-0.01C | 21 ± 3 | [68] |
| Fe-28% Mn-3Al-3Si-0.01C | 41 ± 5 | [68] |

The substantial increase in SFE energy above 25 wt % Mn, as shown in Reference [68] and in Table 1, is consistent with experimental observations showing that there is a sharp reduction in the ε-martensite start temperature for additions of Mn that are above 25 wt % in binary Fe-Mn alloys [70], thereby encouraging twinning, even with this high SFE.

The effect of C is also very important in these high Mn steels (Figure 14b) [64], as it raises the SFE; for a 22% Mn steel with 1–2% Al, an 0.1% increase in C content gives an ~3.5 mJ $m^{-2}$ increase in SFE [71]. Hence, having a low C steel (e.g., 0.1% C), as well as making it difficult to have austenite at room temperature also makes it difficult for the steel to undergo twinning, favoring instead ε martensite formation.

Generally, in TWIP steels, Al or Si, or both are present to yield the required degree of twinning. Although the high level of aluminum content (1–2%) raises the SFE, it has become a favored addition as it prevents hydrogen-delayed fracture in deep-drawn products and, of course, reduces the weight, this being particularly important in the car industry. It also strongly depresses the temperature needed for the ϒ austenite to ε martensite transformation under deformation, encouraging twinning formation [66].

In contrast to Al additions, Si is found to lower the SFE (Figure 14c). For example, an addition of 1.5% Si to a Fe-15%–Mn-1%–Al-0.6% C combination causes the SFE to decrease by ~4 mJ $m^{-2}$ [64], while the same addition of Al to a Si-free–Fe-15%–Mn-0.5% C alloy causes an increase of ~10 mJ $m^{-2}$ [64]. The two elements, Al and Si, are useful for balancing the SFE to the level required for twinning. Although the change in deformation from ϒ to ε martensite is what gives a TRIP steel its good properties, a TWIP steel, in contrast, requires a stable ϒ so that twinning can occur. Of the two methods of strengthening, twinning has been found to give both greater strength and ductility. Although the addition of Al increases the SFE, it is, nevertheless, also very effective in encouraging mechanical twinning rather than phase transformation [72].

In addition to composition having a major influence in controlling the value of the SFE, grain size also has a sizeable effect. Lee and Choi [70] have shown that refining the grain size from 150 to 5 μm causes the SFE to increase by ~10 mJ $m^{-2}$ in Fe–Mn alloys. However, with the coarse grain-size range present after casting, generally 400–1000 μm, such grain-size changes will only result in a very small decrease in the SFE [70], therefore having little effect on twinning behavior.

TWIP steels normally have 15–22% Mn and are generally high in C (0.4–0.6% C). Fe-18%–Mn-0.6% C steel having an SFE value of 24 m $Jm^{-2}$ will comfortably be fully austenitic at room temperature, according to Equation (3). However, it is also important that the composition meets the SFE requirement of ~20–40 mJ $m^{-2}$. The experimental values that have been obtained for the SFE of Fe-18%–Mn-0.6% C TWIP steels range from 13 to 20 mJ $m^{-2}$ [68,69,73]; however, adding 1.5% Al to the steel increases the experimental SFE range to one that is more suitable for the twinning effect at 26–40 mJ $m^{-2}$ [69,74,75]. Zambrano [64] has noted that his theoretical calculations fit well with the experimental values for the SFE.

In contrast to Al additions, which increase the SFE, Jeong et al. found that adding 1.5% Si reduced the experimental SFE from 19 to 14 mJ $m^{-2}$ [73]. Again, these experimental values fitted in reasonably well with Zambrano's theoretical thermodynamic calculations [64].

A more economical way of producing TWIP steel would be to reduce the Mn and compensate for this by adding Si or increasing the carbon level.

In addition to obtaining a suitable SFE, a fully austenitic structure is needed at room temperature; to achieve this often means having a C level as high as 0.6% C, as well as a high Mn level. The compositional window for obtaining TWIP steel is, therefore, relatively narrow, as it has to meet the required stacking fault energy and also ensure that the steel is fully austenitic at room temperature.

The SFE is also important for the overall hot ductility performance; the lower the SFE, the more difficult dislocation cross-slip becomes, so that dislocations accumulate in the un-recrystallized grains, favoring DRX [76].

However, although DRX is important when it comes to hot-working, where the strains are high, this is not the case for the straightening operation, where the strain is very low (1–3%). Unfortunately for assessing the cracking susceptibility on straightening, the hot tensile test normally realizes sufficiently high strains on testing to lead to DRX. As mentioned earlier, this gives unrealistically high RA values for the straightening operation, so care has to be taken when applying the results from a hot tensile test, to assess the likelihood of cracking on straightening.

Although these small additions are unlikely to have any major influence on the SFE, certainly, by the time they reach a 1% level, as with Al, Si, Cu, and Ni, they will have a significant influence and will then influence the material's properties.

## 5. Influence of Cerium on Hot Ductility

Because of the problem of continuously casting these highly alloyed steels without cracks forming, particularly in the case of high-Al TWIP and TRIP steels, and the need to add B to be able to achieve this effect, other microalloying additions should also be considered.

A rare-earth addition of cerium is likely to be a good candidate for improving the hot ductility of these steels, having many benefits such as being able to deoxidize, refine the grain size, remove S from solution, and prevent hydrogen-cracking [77–79]. Kim et al. [80] have found that the addition of Ce (0.017–0.027%) is very effective in combating HICC (hydrogen-induced cold cracking) or delayed fracture in welded joints because the oxide particles give sufficient trapping efficiency to effectively reduce the diffusible hydrogen content.

Since the 1960s, rare earth additions (Misch metal) have been used to improve the fracture toughness of HSLA steels, through their ability to modify the shape after hot rolling, from elongated MnS inclusions to hard globular Ce complex sulfides [78]. This was particularly important for the through-the-thickness fracture performance of line-pipe and oil-platform steels.

Much of the recent research has been centered on the mode of cerium inclusion development during the solidification of these steels. In HSLA steels, the typical small globular inclusions (<5 μm) are of Ce-O, which gradually change to Ce-O-S, and, finally, to CeS with increasing Ce content [81]. The cause of the finer austenite grain size or dendrite size after adding Ce is not always clear, but, as with Nb, it is either due to precipitation pinning the boundaries or a solute drag effect.

Recently, it has been shown that when Ce is added to the melt in Al-killed grade SS400 mild steel (0.2% C, 1.4% Mn, 0.4% Si, low S, and P), the $Ce_2O_2S$ inclusions that formed, which were 5–7 μm in size, served as heterogeneous nucleation sites for the desired intergranular acicular ferrite structure [82].

Although cerium's ability to grain-refine and improve the hot ductility of plain C-Mn and HSLA is well-documented [65], there is little information on using Ce to improve the hot ductility of AHSS steels specifically, but what information is available from the past literature looks very promising. A recent paper by Li et al. [83], concentrating on the solidification processes, shows that Ce will refine the solidification structure and, although no hot ductility work was carried out, it is likely that ductility will, in consequence, improve. TWIP steels are prone to having an uneven grain size, due to inhomogeneous

solute distribution, and suffer from micro-porosity, meaning that Ce would seem to be an excellent solution [84,85]. This inhomogeneous solute distribution can also lead to the early fracture of TWIP steels [86].

Again, Ce additions to cryogenic vessel steels have been shown to improve the cleanliness and quality of the steel and, most importantly, reduced the center line segregation with an addition as low as 0.001% [87,88]. Coarse dendritic grains and micro-segregation have been suggested as a major cause of the poor ductility seen after casting [82–86], so Ce may be very beneficial for preventing cracking.

In Li et al.'s work [83], the solidification structures of an Fe-22Mn-0.6C-1.6Al TWIP steel with Ce additions from 0.06 to 0.26% were examined. They concluded that in the range of 0.05–0.18%, Ce expanded the equiaxed zone, giving a 50% reduction in the equiaxed grain size on solidification, compared with steel of similar composition that contained no Ce. The $CeO_2$ particles were regarded as being responsible for this grain refinement. The dendritic arms were also thinner; this refinement was ascribed to solute drag from the Ce. The equilibrium partition coefficient of Ce in steel is ~0.02–0.04 [88], indicating a strong tendency to segregate during solidification. Although this work has concentrated on the solidification structures rather than hot ductility, their results suggest that ductility will be very much enhanced by the addition of Ce. This is confirmed by recent papers [89,90] in which Ce has been added to low-C alloyed steels for reactor pressure vessels. Ductility was found to improve throughout the hot ductility curve when an addition of ~ 0.07% Ce was made (Figure 15) [89]. A fairly conventional processing route for hot ductility testing was used, in which tensile specimens from plate steel were heated to 1300 °C and cooled to the test temperatures shown in Figure 15. A trough was obtained, covering the temperature range of 700–850 °C, in which a thin film of ferrite was present. The presence of DRX was first noticed at 950 °C.

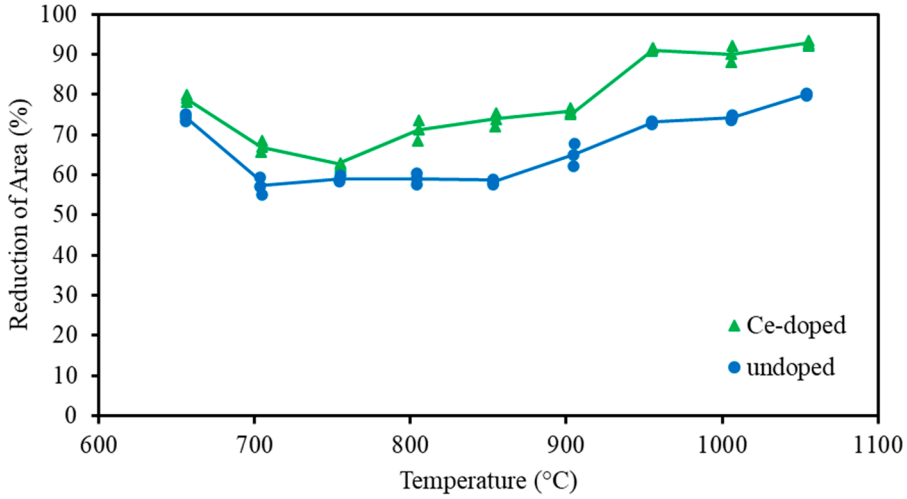


**Figure 15.** The hot ductility curves of reactor pressure-vessel steel that is both un-doped and doped with 0.07% Ce. The base composition of the steel was 0.18% C, 0.22% Si, 1.45% Mn, 0.75% Ni, and 0.5% Mo [89]. Adapted from [89], with permission from Elsevier, 2023.

The segregation of Ce to the boundaries was confirmed and they suggest that this may have enhanced the grain boundary cohesion, restraining grain boundary sliding. This 10–15% improvement in RA values over a very wide temperature range does seem to be a feature when segregation is responsible for the improvement. The ductility for the steel was, nevertheless, very good even in the un-doped steel, being > 50% over the entire testing range (Figure 15). However, Guo et al. [89] considered this ductility to be poor, mistakenly taking >60% as the requirement to avoid cracking. Indeed, many authors have misquoted this requirement, referring to papers by Mintz et al. [1,6,21,24,36,37,39,52] that have never mentioned this criterion, and who quote 35–40% RA as the acceptable level.

Guo et al. [90] have also shown that Ce improves the ductility of a more highly alloyed reactor pressure vessel steel, which was fully austenitic throughout the testing temperature range of 700–1000 °C. In this case, adding 0.045% P improved the ductility in the temperature range of 750–850 °C (Figure 16). A further improvement occurred when adding Ce, so that the trough was entirely removed. Both Ce and P were shown to segregate to the boundaries. It was suggested that by segregating to the boundaries, P restrained GBS; it also favored DRX, which occurred at temperatures in the range of 850–900 °C. The influence of P on hot ductility is confusing and it is not a favored addition because it causes embrittlement at room temperature. However, because it segregates to the boundaries and probably removes micro-voids, making it more difficult for GBS to occur, it could improve hot ductility; however, this is only the case, provided that the low melting-point iron phosphide phases do not form. Since the improvement was credited to DRX, as has been noted in the earlier review [1], this is not relevant to the straightening operation [1].

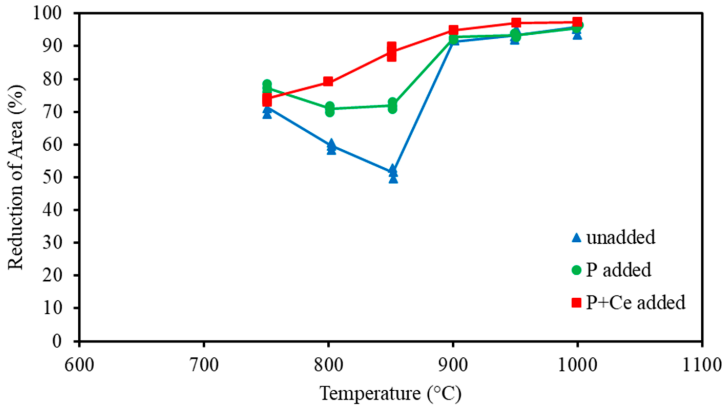


**Figure 16.** Hot ductility curves for low C, low Mn, 3% Ni, 1.75% Cr, 0.5% Mo material, having: no additions of P and Ce, a 0.045% P addition, and a 0.045% P, 0.03% Ce addition [90].

Earlier work by Song et al. [22] again showed how important trace elements can be in hot ductility, by segregating to the boundaries and influencing the cohesion. In this case, in contrast to Ce, when Sn is added, the segregation of Sn to the boundaries reduces cohesion (Figure 17). Again, ductility is restored when Ce is added. It was suggested that Ce strengthens the grain-boundary regions when the film of ferrite is present, as well as in the austenite, thereby restraining GBS. Ce was also shown to delay the formation of the ferrite film [22].

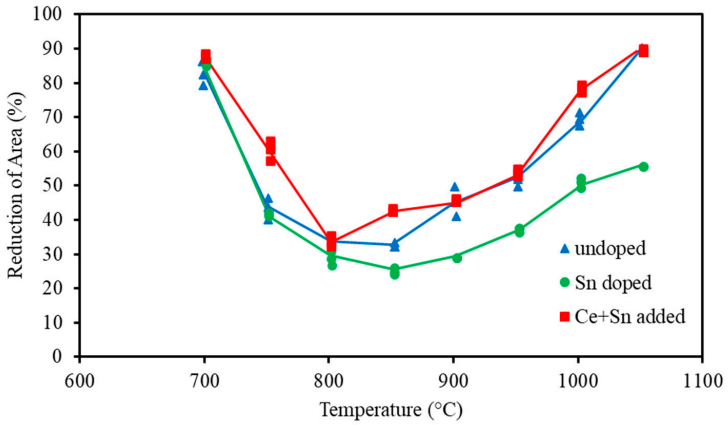


**Figure 17.** Hot ductility curves for 0.1% C, 1% Cr, 0.5 % Mo steels that were un-doped, doped with 0.055% Sn, and doped with 0.055% Sn and 0.05% Ce [22]. Adapted from [22], with permission from Elsevier, 2023.

Obviously, more work is required to establish the benefits of Ce addition, but the results from the work to date do seem to be encouraging. However, it should be noted that although Ce has been shown to refine the solidification structure [83], a new and exciting solution to the problem of cracking in these steels has just been published, in which MnS inoculation into the melt has been used to refine the solidification structure, leading to a significant improvement in hot ductility. This may prove to be a cheaper route [91].

## 6. Influence of Cu and Ni on Hot Ductility

Cu, unless it is accompanied by Ni, is not normally added to steels because of the problem of hot shortness, except for weathering steels, when Si can be added because of its protective oxide surface scale. However, both elements are austenite stabilizers and can increase hardenability; they have been suggested as additions for TRIP and even TWIP steels [3,92–96]. Cu is considered to be a good addition to make to TRIP and DP steels because, as well as its ability to stabilize the austenite and thus decrease the work-hardening rate, so that the martensite reaction takes place at a later stage, enabling higher elongations and strength to be attained [3], it also has a moderate solid solution-hardening effect and it can grain-refine via solute drag and thereby retard recrystallization. Cu additions can also precipitate out as ductile copper particles, which can bestow considerable strengthening capability and improve the fracture toughness when age-hardened at 400–500 °C [97,98]. Both elements increase the SFE and so encourage cross-slip; therefore, a build-up of dislocations does not occur [99,100].

As far as the straightening operation is concerned, small Cu additions do not influence the hot ductility curves for normal testing conditions; however, when the conditions are closer to the commercial situation, i.e., casting the tensile specimens in an oxidizing atmosphere, the ductility decreases and cracking can occur, even at as low a level of Cu as 0.2%. Nevertheless, if Ni is added, the solubility of Cu in austenite increases, so that pure Cu cannot precipitate out and melt along the austenite grain boundaries, leading to intergranular failure. An equal amount of Ni will often be sufficient [101].

Cu additions of 1–2% have been suggested for TRIP steels [3,92] bestowing considerable strengthening capacity. TWIP steels can similarly benefit from this addition [96].

## 7. Influence of Ca and Zr on Hot Ductility

Although both Ca and Zr have been suggested as microalloying additions to improve hot ductility, there is only limited experimental hot ductility testing that has been carried out on these steels [18,21].

Both of these elements bear many similarities to Ce in being able to deoxidize and de-sulfurize. Ca is added to improve the "cleanliness" of steels, by reducing the S level and modifying the inclusions into a globular shape, so that the room-temperature fracture strength is improved, particularly in the through-the-thickness direction in plate steel [102]. It is also an important addition during secondary steelmaking with Al-killed steels, to prevent the nozzle from clogging with the solid alumina oxides by forming liquid calcium aluminate [103]. This liquid window, however, disappears when too much Ca is added, and solid CaS is formed. The amount of Ca required is mainly controlled by the sulfur content of the steel. The modification of the soft MnS inclusions, which elongate out with rolling to the harder CaMn sulfides and remain spherical on rolling, gives an impressive increase in fracture toughness, along with the higher shelf energies on impact transition curves. Having such cleanliness is particularly important for achieving good properties in AHSS steels [104].

Zr is highly reactive and combines readily with oxygen, nitrogen, sulfur, and carbon in decreasing order of reactivity [105]. Its use in steelmaking over Ca is that it can remove S and $O_2$ more effectively; also, because it forms a nitride, it can be particularly useful in boron-treated steels, preventing boron nitride from forming at the boundaries.

In early work by Mintz et al. [21], the influence of a Ca addition on hot ductility was examined by tensile testing by casting in situ, Figure 18a as well as after solution-treating

at 1300 °C, Figure 18b. In all cases, small Ca additions (0.004% Ca) were found to improve the hot ductility performance (Figure 18a,b). Ca was shown to be very beneficial to the hot ductility of plain C-Mn steels and Nb-containing HSLA steels by encouraging DRX and thereby narrowing the trough, and, more importantly, for preventing transverse cracking in decreasing the depth of the trough, as shown in Figure 18b which gives the curves for the plain C-Mn steels. Only the curves for the plain C-Mn steels are given; the Nb-containing steels displayed similar behavior but the curves were displaced to lower RA values, due to the additional dynamic precipitation by Nb(CN). MnS inclusions have been found to prevent DRX by pinning the austenite grain boundaries, this being a favored nucleation site, as S readily segregates to the boundaries. Hence, the reduction in the number of sulfides by Ca treatment encourages DRX. One consequence of encouraging DRX is to narrow the ductility trough, as well as reduce its depth [1,24].

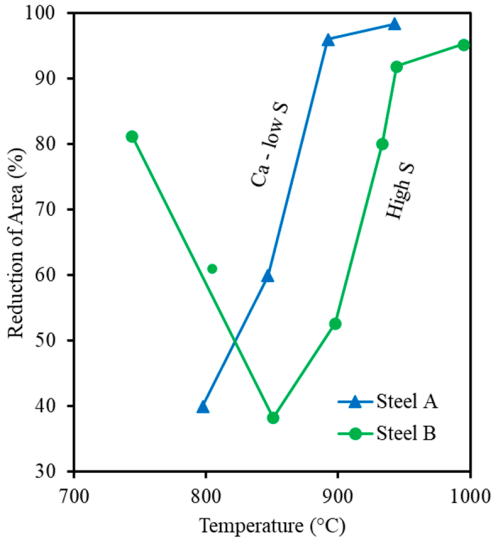


(**a**)

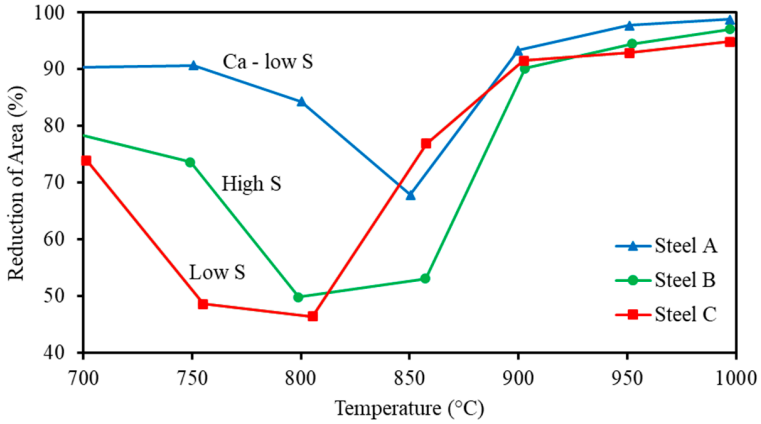


(**b**)

| Steel | C% | Si% | Mn% | P% | S% | Al% | N% | Ca% |
|---|---|---|---|---|---|---|---|---|
| A | 0.07 | 0.5 | 1.45 | 0.007 | 0.004 | 0.04 | 0.007 | 0.004 |
| B | 0.06 | 0.4 | 1.45 | 0.007 | 0.012 | 0.03 | 0.007 | - |
| C | 0.11 | 0.3 | 1.45 | 0.011 | 0.002 | 0.04 | 0.004 | - |

(**c**)

**Figure 18.** Hot ductility curves for steels with and without Ca additions. (**a**) steels cast in situ, (**b**), Solutions treated at 1300 °C (**c**) a table giving the composition of the steels [21]. Adapted from [21], with permission from Taylor & Francis Group, 2022.

These authors raised the important point that it is the S in solution at 1330 °C, rather than the total S content, that is important in controlling the hot ductility performance. This controls the volume fraction of sulfides, which are precipitated at the austenite grain boundaries on cooling to the test temperature. Calcium sulfides do not go back into a solution as easily as MnS at 1330 °C, therefore the S level in the solution will be lower, resulting in fewer sulfides on cooling to the test temperature. Hence, for Ca-free steels (see the table of compositions in Figure 18c), there is little difference in hot ductility in terms of raising the sulfur level from 0.004% to 0.012% for tensile specimens heated to 1330 °C, Figure 18b, except the curve for the low S steel is moved to lower temperatures due to its higher C content (0.05% higher C). Even the low S-containing steel, (C) has poor ductility compared to that shown by the Ca-treated steel (A) (Figure 18b). However, even when the sulfides are MnS, only 0.001% of S goes back into a solution at 1330 °C when the Mn

content is 1.4% Mn; this is independent of the total S-levels in the steel [106]. Hence, there is little difference in the hot ductility curves for the "high and low S" steel (Figure 18b) except for the C level being higher in the low-S steel; the transformation from austenite to ferrite is lowered, so that the curve moves to lower temperatures.

In contrast, in the as-cast condition (Figure 18a), the total S is available for precipitating out after cooling to the test temperature, so that the ductility is very sensitive to the total S level. As Ca is so effective in removing S, it is now very beneficial to the hot ductility, and, hence, there is a difference in hot ductility between lower and higher S-containing steels (Figure 18a).

However, more recent work by Taguchi et al. [47] has also shown that Ca does improve ductility at the high-temperature end of the trough (> 800 °C) in B-treated steel, but this is only by a very small amount (Figure 19). Although B can be very effective in improving the hot ductility, if given the right secondary-cooling conditions, it is not always possible to achieve this, and there is always the danger of a fine precipitation of BN forming at the austenite grain boundaries, preventing DRX and leading to ductile intergranular failure. The calcium sulfides act as favored precipitation sites for BN to precipitate out on, instead of precipitating at the austenite grain boundaries. The very low sulfur level (0.003%) in the steels, prior to Ca treatment, may explain the rather small improvement shown in Figure 19 that is noted after Ca treatment.

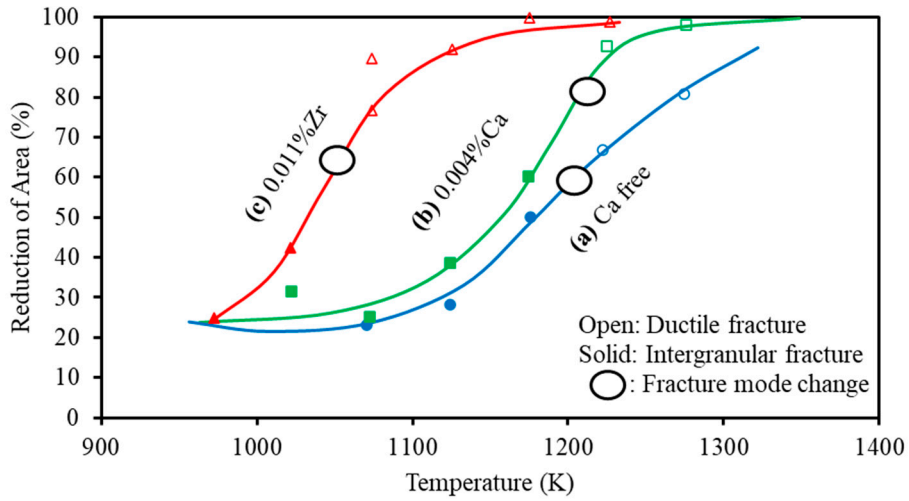


**Figure 19.** Relationship between tensile temperature and reduction in area for steel with a base composition of ~0.1% C, 0.15% Si, 1.4% Mn, 0.01% Ti, 0.0017% B, < 0.0001% P, 0.003% S, 0.005% N, and 0.011% Al, (**a**) Ca-free, (**b**) 0.004% Ca, and (**c**) 0.011% Zr [47]. The symbol O on the curves marks the changeover from intergranular failure to ductile failure.

In this work [47], the tensile specimens were melted, cooled at 600 °C/min to 1250 °C, and then cooled at 24 °C/min to the test temperature. Finally, they were strained to failure using a strain rate of $3 \times 10^{-4}$ $s^{-1}$. Although the Ca addition had only a small influence on hot ductility, Zr was very beneficial, Figure 19. This arises because Zr, unlike Ca, is a very strong nitride former and, similar to Ti, protects the boron from precipitating as a nitride at the boundaries by taking the nitrogen out of the solution, whence it can be removed in the melt.

The Ca/S ratio is also very important for realizing improvements in hot ductility. Karjalainen et al. [107] found that in the case of HSLA steels, increasing the Ca/S ratio (a Ca range of 0 to 0.005% Ca and a S range of 0.004 to 0.009% S) caused the RA value at the temperature showing the minimum ductility in the trough, 750 °C, to significantly increase. This improvement was even more noticeable as the cooling rate decreased from 240 to 24 °C/min.

The works of Coleman and Wilcox [108] and Suzuki et al. [18] are probably the most definitive in clarifying the role of these elements in influencing the likelihood of transverse cracking occurring, being based on both experimental hot ductility tests and commercial experience of cracking from their published data. Their conclusions were that for cast HSLA slabs, the addition of Ca and/or Ce by precipitating out the S as sulfides in the liquid, along with Ti and/or Zr, by precipitating out nitrides in the liquid, resulted in crack-free slabs. The beneficial influence of adding Zr is clearly shown in Figure 20 as AlN is not able to form, nor are the niobium carbo-nitrides.

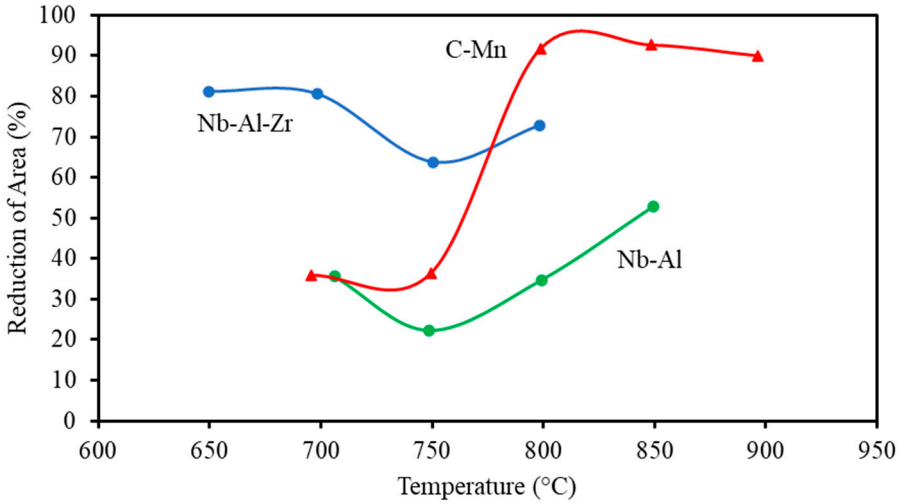


**Figure 20.** Hot ductility curves for plain C-Mn, C-Mn-Nb-Al, and C-Mn-Nb-Al-Zr steels. Tensile samples were solution-treated at 1330 °C, then cooled to the test temperature at 60 °C/min and strained at a rate of $3 \times 10^{-3}$ $s^{-1}$ [108], with the permission from Taylor & Francis, 2023.

## 8. Conclusions

1. Small additions of Cr have little influence on hot ductility and, at the 0.5% level, deteriorate ductility, while Mo, at values up to 0.5%, has been shown to be beneficial to the hot ductility on straightening for TRIP-assisted steels. Mo is particularly useful in these steels as it encourages bainite formation and, provided the cooling rate is fast enough, can avoid ferrite transformation. The two elements increase hardenability so that lower C contents can be used to produce the retained austenite needed to achieve their excellent room-temperature combination of strength and ductility.

2. Provided that it is well protected by Ti and the cooling conditions are within the range of 10–100 °C/min, by segregating to the boundaries, boron can strengthen them during the straightening operation. Slower cooling rates are recommended to coarsen the TiN precipitates. The benefits of boron addition to hot ductility apply to both TRIP-assisted and TWIP steels, but it has been found to be particularly valuable for improving the hot ductility on straightening for the high Al and high Mn TWIP steels.

3. Copper and nickel are both austenite stabilizers; therefore, they can be very useful in improving the properties of TRIP-assisted steels. They both increase the hardenability. Copper, provided that Ni is added to prevent hot shortness, has been found to be particularly useful as an addition to these AHSS steels, for, as well as increasing the strength, it can also improve the fracture toughness. Nickel also appears to be able to coarsen carbides and can thus improve the hot ductility performance.

4. Ce has not received the attention it deserves; it seems to behave very similarly to boron but does not form a carbide or nitride and fulfills an additional task of removing sulfides and oxides from the melt.

5. As with Ce, Ca is very good at removing sulfur and so can improve the hot ductility performance. The element is also very good at preventing nozzle blockage caused by the hard alumina particles, by converting them to liquid calcium aluminate.

6. Zr also seems to be a good element to add, as it desulfurizes, deoxidizes, and is a very strong nitride former; as with Ti, it can also protect boron from forming boron nitride precipitates at the austenite grain boundaries.

**Author Contributions:** Conceptualization: B.M.; Methodology: B.M.; Writing—review and Editing: B.M. and A.Q.; Writing—original draft preparation: B.M. and A.Q.; Supervision: B.M. and S.E.K.; Project Administration: B.M. and S.E.K. All authors have read and agreed to the published version of the manuscript.

**Funding:** This research received no external funding.

**Data Availability Statement:** Data presented in this article are available at request from the corresponding author.

**Conflicts of Interest:** The authors declare no conflict of interest.

## References

1. Mintz, B.; Qaban, A. The Influence of Precipitation, High Levels of Al, Si, P and a Small B Addition on the Hot Ductility of TWIP and TRIP Assisted Steels: A Critical Review. *Metals* **2022**, *12*, 502. [CrossRef]
2. Andrews, K.W. Empirical formulae for the calculation of some transformation temperatures. *J. Iron Steel Inst.* **1965**, *7*, 721–727.
3. Allain, S.; Iung, T. Development of hot rolled copper/nickel alloyed TRIP steels with carbide-free bainitic matrix. *Metall. Res. Technol.* **2008**, *105*, 520–530. [CrossRef]
4. Kwon, O.; Kim, S.; Cho, J.; Kwak, W.; Kim, G. Development of TWIP steel for automotive application, Posco, Korea. In Proceedings of the 3rd International Steel Conference on New Developments in Metallurgical Process Technologies (METEC InSteelCon), Düsseldorf, Germany, 11–15 June 2007; pp. 690–697.
5. Horvath, C.D. Advanced steels for lightweight automotive structures. In *Materials, Design and Manufacturing for Lightweight Vehicles*; Woodhead Publishing: Sawston, UK, 2021; pp. 39–95.
6. Mintz, B. Hot dip galvanising of transformation induced plasticity and other intercritically annealed steels. *Int. Mater. Rev.* **2001**, *46*, 169–197. [CrossRef]
7. Mesplont, C.; Waterschoot, T.; Vandeputte, S.; De Cooman, B.C. *Thermomechanical Processing of Steels*; IoM Communications: London, UK, 2000; Volume 2, pp. 495–504.
8. Kucerova, L.; Bystrianský, M. The effect of chemical composition on microstructure and properties of TRIP steels. *J. Achiev. Mater. Manuf. Eng.* **2016**, *77*, 5–12. [CrossRef]
9. Uranga, P.; Shang, C.-J.; Senuma, T.; Yang, J.-R.; Guo, A.-M.; Mohrbacher, H. Molybdenum alloying in high-performance flat-rolled steel grades. In Proceedings of the 2018 Molybdenum and Steel Symposium (IMOA), Shanghai, China, 28–29 November 2018; pp. 5–23. [CrossRef]
10. Liu, Y.; Sun, Y.-H.; Wu, H.-T. Effects of chromium on the microstructure and hot ductility of Nb-microalloyed steel. *Int. J. Miner. Met. Mater.* **2021**, *28*, 1011–1021. [CrossRef]
11. Hannerz, N. Critical hot plasticity and transverse cracking in continuous slab casting with particular reference to composition. *Trans. Iron Steel Inst. Jpn.* **1985**, *25*, 149–158. [CrossRef]
12. Zheng, Y.; Shen, W.; Zhu, L.; Guo, Z.; Wang, Q.; Feng, J.; Li, Y.; Cao, R.; Wu, J. Effects of composition and strain rate on hot ductility of Cr–Mo-alloy steel in the two-phase region. *High Temp. Mater. Process.* **2021**, *40*, 228–240. [CrossRef]
13. Mejía, I.; Salas-Reyes, A.E.; Bedolla-Jacuinde, A.; Calvo, J.; Cabrera, J.M. Effect of Nb and Mo on the hot ductility behavior of a high-manganese austenitic Fe–21Mn–1.3 Al–1.5 Si–0.5 C TWIP steel. *Mater. Sci. Eng. A* **2014**, *616*, 229–239. [CrossRef]
14. Banerji, S.K.; Morral, J.E. *Boron in Steel*; AIME: Milwaukee, WI, USA, 1979; p. 1980.
15. Azarkevich, A.A.; Kovalenko, L.V.; Krasnopolskii, V.M. The optimum content of boron in steel. *Met. Sci. Heat Treat.* **1995**, *37*, 22–24. [CrossRef]
16. Cameron, T.B.; Morral, J.E. The solubility of boron in iron. *Met. Mater. Trans. A* **1986**, *17*, 1481–1483. [CrossRef]
17. Shen, Y.; Hansen, S.S. Effect of the Ti/N ratio on the hardenability and mechanical properties of a quenched-and-tempered C-Mn-B steel. *Met. Mater. Trans. A* **1997**, *28*, 2027–2035. [CrossRef]
18. Suzuki, K.-I.; Miyagawa, S.; Saito, Y.; Shiotani, K. Effect of Microalloyed Nitride Forming Elements on Precipitation of Carbonitride and High Temperature Ductility of Continuously Cast Low Carbon Nb Containing Steel Slab. *ISIJ Int.* **1995**, *35*, 34–41. [CrossRef]
19. Abushosha, R.; Vipond, R.; Mintz, B. Influence of titanium on hot ductility of as cast steels. *Mater. Sci. Technol.* **1991**, *7*, 613–621. [CrossRef]
20. Abushosha, R.; Comineli, O.; Mintz, B. Influence of Ti on hot ductility of C–Mn–Al steels. *Mater. Sci. Technol.* **1999**, *15*, 278–286. [CrossRef]
21. Mintz, B.; Mohamed, Z.; Abu-Shosha, R. Influence of calcium on hot ductility of steels. *Mater. Sci. Technol.* **1989**, *5*, 682–688. [CrossRef]
22. Shenhua, S.; Yewei, X.U.; Xianmiao, C.; Jiang, X. Effect of rare earth cerium and impurity tin on the hot ductility of a Cr-Mo low alloy steel. *J. Rare Earths* **2016**, *34*, 1062–1068.

23. López-Chipres, E.; Mejía, I.; Maldonado, C.; Bedolla-Jacuinde, A.; Cabrera, J. Hot ductility behavior of boron microalloyed steels. *Mater. Sci. Eng. A* **2007**, *460–461*, 464–470. [CrossRef]
24. Mintz, B.; Qaban, A. Understanding the high temperature side of the hot ductility curve for steels. *Mater. Sci. Technol.* **2021**, *37*, 237–249. [CrossRef]
25. Lagerquist, M.; Lagneborg, R. The influence of boron on the creep properties of austenitic steels. *Scand. J. Metall.* **1972**, *1*, 81–89.
26. Khadkikar, P.S.; Vedula, K.; Shabel, B.S. Role of boron in ductilizing $Ni_3Al$. *Metall. Trans. A Phys. Metall. Mater. Sci.* **1987**, *18*, 425–428. [CrossRef]
27. Mavropoulos, T.; Jonas, J.J.; Ruddle, G.E. HSLA Steels: Metallurgy and Applications. In Proceedings of the International Conference on HSLA Steels' 85, Beijing, China, 4–8 November 1985; p. 229.
28. Jahazi, M.; Jonas, J. The non-equilibrium segregation of boron on original and moving austenite grain boundaries. *Mater. Sci. Eng. A* **2002**, *335*, 49–61. [CrossRef]
29. Cao, B.; Wang, X.; Cui, H.; He, X. Non-equilibrium segregation of boron on grain boundary in Fe-30% Ni alloy. *Int. J. Miner. Metall. Mater.* **2002**, *9*, 347–351.
30. Kim, S.K.; Kim, N.J.; Kim, J.S. Effect of boron on the hot ductility of Nb-containing steel. *Met. Mater. Trans. A* **2002**, *33*, 701–704. [CrossRef]
31. Song, S.-H.; Guo, A.-M.; Shen, D.-D.; Yuan, Z.-X.; Liu, J.; Xu, T.-D. Effect of boron on the hot ductility of 2.25Cr1Mo steel. *Mater. Sci. Eng. A* **2003**, *360*, 96–100. [CrossRef]
32. Campbell, J. Discussion of "Investigation of Oxide Bifilms in Investment Cast Superalloy IN100 Parts I and II"*. *Met. Mater. Trans. A* **2017**, *48*, 5151–5153. [CrossRef]
33. Campbell, J. Melting, remelting, and casting for clean steel. *Steel Res. Int.* **2017**, *88*, 1–13. [CrossRef]
34. Song, S.-H.; Faulkner, R.G.; Flewitt, P.E.J. Effect of boron on phosphorus-induced temper embrittlement. *J. Mater. Sci.* **1999**, *34*, 5549–5556. [CrossRef]
35. Grabke, H.J. *Impurities in Engineering Materials*; Briant, C.L., Ed.; Marcel Dekker: New York, NY, USA, 1999; Volume 143, p. 192.
36. Mintz, B.; Tuling, A.; Delgado, A. Influence of silicon, aluminium, phosphorus and boron on hot ductility of TRansformation Induced Plasticity assisted steels. *Mater. Sci. Technol.* **2003**, *19*, 1721–1726. [CrossRef]
37. Mintz, B.; Yue, S.; Jonas, J.J. Hot ductility of steels and its relationship to the problem of transverse cracking during continuous casting. *Int. Mater. Rev.* **1991**, *36*, 187–220. [CrossRef]
38. Salas-Reyes, A.E.; Altamirano-Guerrero, G.; Chávez-Alcalá, J.F.; Barba-Pingarrón, A.; Figueroa, I.A.; Bolarín-Miró, A.M.; Jesús, F.S.-D.; Deaquino-Lara, R.; Salinas, A. Influence of Boron Content on the Solidification Structure, Magnetic Properties and Hot Mechanical Behavior in an Advanced As-Cast TWIP Steel. *Metals* **2020**, *10*, 1230. [CrossRef]
39. Mintz, B.; Kang, S.; Qaban, A. The influence of grain size and precipitation and a boron addition on the hot ductility of a high Al, V containing TWIP steels. *Mater. Sci. Technol.* **2021**, *37*, 1035–1046. [CrossRef]
40. Zarandi, F.; Yue, S. The Effect of Boron on Hot Ductility of Nb-microalloyed Steels. *ISIJ Int.* **2006**, *46*, 591–598. [CrossRef]
41. Mejía, I.; Salas-Reyes, A.E.; Calvo, J.; Cabrera, J.M. Effect of Ti and B microadditions on the hot ductility behavior of a High-Mn austenitic Fe–23Mn–1.5 Al–1.3 Si–0.5 C TWIP steel. *Mater. Sci. Eng. A* **2015**, *648*, 311–329. [CrossRef]
42. Nix, W.D.; Yu, K.S.; Wang, J.S. The effects of segregation on the kinetics of irrtergranular cavity growth under creep conditions. *Met. Mater. Trans. A* **1983**, *14*, 563–570. [CrossRef]
43. Laha, K.; Kyono, J.; Kishimoto, S.; Shinya, N. Beneficial effect of B segregation on creep cavitation in a type 347 austenitic stainless steel. *Scr. Mater.* **2005**, *52*, 675–678. [CrossRef]
44. Yamamoto, K.; Suzuki, H.G.; Oono, Y.; Noda, N.; Inoue, T. Formation Mechanism and Prevention Method of Facial Cracks of Continuously Cast Steel Slabs Containing Boron. *Tetsu-To-Hagane* **1987**, *73*, 115–122. [CrossRef]
45. Cho, K.C.; Mun, D.J.; Kim, J.Y.; Kil Park, J.; Lee, J.S.; Koo, Y.M. Effect of Boron Precipitation Behavior on the Hot Ductility of Boron Containing Steel. *Met. Mater. Trans. A* **2010**, *41*, 1421–1428. [CrossRef]
46. Wang, W.S.; Zhu, H.Y.; Sun, J.; Lei, J.L.; Duan, Y.Q.; Wang, Q. Thermodynamic analysis of BN, AlN and TiN precipitation in boron-bearing steel. *Metalurgija* **2019**, *58*, 199–202.
47. Taguchi, K.; Takaya, S.; Numata, M.; Kato, T. Effect of Deoxidizing Element on the Hot Ductility of Boron-Containing Steel. *ISIJ Int.* **2020**, *60*, 2829–2837. [CrossRef]
48. Tingdong, X.; Shenhua, S.; Zhexi, Y.; Zongsen, Y. Two types of boron segregation at austenite grain boundaries and their mutual relation. *J. Mater. Sci.* **1990**, *25*, 1739–1744. [CrossRef]
49. Shenhua, S.; Tingdong, X.; Zhexi, Y.; Zongsen, Y. Equilibrium grain-boundary segregation and the effect of boron in B-doped Fe−3wt%Ni austenitic alloy. *Acta Met. Mater.* **1991**, *39*, 909–914. [CrossRef]
50. He, X.; Chu, Y.; Jonas, J. Grain boundary segregation of boron during continuous cooling. *Acta Met.* **1989**, *37*, 147–161. [CrossRef]
51. Karlsson, L. Non-equilibrium grain boundary segregation of boron in austenitic stainless steel-III. Computer simulations. *Acta Metall.* **1988**, *36*, 1–12. [CrossRef]
52. Mintz, B.; Crowther, D.N. Hot ductility of steels and its relationship to the problem of transverse cracking in continuous casting. *Int. Mater. Rev.* **2010**, *55*, 168–196. [CrossRef]
53. Shen, K.; Wang, S.F.; Ma, H.; Liao, S.L. Analysis and improving measures for surface defects on low carbon boron steel. *J. Iron Steel Res.* **2014**, *26*, 57–62.

54. Cho, K.C.; Mun, D.J.; Kang, M.H.; Lee, J.S.; Kil Park, J.; Koo, Y.M. Effect of Thermal Cycle and Nitrogen Content on the Hot Ductility of Boron-bearing Steel. *ISIJ Int.* **2010**, *50*, 839–846. [CrossRef]
55. Chown, L.; Cornish, L. Investigation of hot ductility in Al-killed boron steels. *Mater. Sci. Eng. A* **2008**, *494*, 263–275. [CrossRef]
56. Tanino, M. Precipitation behaviours of complex boron compounds in steel. Nippon steel technical report. *Overseas* **1983**, *21*, 331–337.
57. Lis, A.; Lis, J.; Kolan, C.; Knapiński, M. Effect of strain rate on hot ductility of C-Mn-B steel. *J. Achiev. Mater. Manuf. Eng.* **2010**, *41*, 26–33.
58. Mejía, I.; Bedolla-Jacuinde, A.; Maldonado, C.; Cabrera, J. Hot ductility behavior of a low carbon advanced high strength steel (AHSS) microalloyed with boron. *Mater. Sci. Eng. A* **2011**, *528*, 4468–4474. [CrossRef]
59. Wilson, F.G.; Gladman, T. Aluminium nitride in steel. *Int. Mater. Rev.* **1988**, *33*, 221–286. [CrossRef]
60. Qaban, A.; Mintz, B.; Kang, S.E.; Naher, S. Hot ductility of high Al TWIP steels containing Nb and Nb-V. *Mater. Sci. Technol.* **2017**, *14*, 1645–1656. [CrossRef]
61. Banks, K.M.; Tuling, A.; Mintz, B. Influence of V and Ti on hot ductility of Nb containing steels of peritectic C contents. *Mater. Sci. Technol.* **2011**, *27*, 1309–1314. [CrossRef]
62. Smallman, R.E.; Dillamore, I.L.; Dobson, P.S. The Measurement of Stacking Fault Energy. *J. Phys. Colloq.* **1966**, *27*, C3-86–C3-93. [CrossRef]
63. Monsalve, A.; De Barbieri, F.; Gómez, M.; Artigas, A.; Carvajal, L.; Sipos, K.; Bustos, O.; Pérez-Ipiña, J. Mechanical Behavior of a Twip Steel (Twinning Induced Plasticity). *Matéria* **2015**, *20*, 653–658. [CrossRef]
64. Zambrano, O.A. Stacking fault energy maps of Fe–Mn–Al–C–Si steels: Effect of temperature, grain size, and variations in compositions. *J. Eng. Mater. Technol.* **2016**, *138*, 041010. [CrossRef]
65. Grässel, O.; Krüger, L.; Frommeyer, G.; Meyer, L.W. High strength Fe–Mn–(Al, Si) TRIP/TWIP steels development—Properties—Application. *Int. J. Plast.* **2000**, *16*, 1391–1409. [CrossRef]
66. Sato, K.; Ichinose, M.; Hirotsu, Y.; Inoue, Y. Effects of deformation induced phase transformation and twinning on the mechanical properties of austenitic Fe-Mn-Al alloys. *ISIJ Int.* **1989**, *29*, 868–877. [CrossRef]
67. Lee, S.J.; Fujii, H.; Ushioda, K. Thermodynamic calculation of the stacking fault energy in Fe-Cr-Mn-CN steels. *J. Alloys Compd.* **2018**, *749*, 776–782. [CrossRef]
68. Pierce, D.T.; Jiménez, J.A.; Bentley, J.; Raabe, D.; Oskay, C.; Wittig, J.E. The influence of manganese content on the stacking fault and austenite/ε-martensite interfacial energies in Fe–Mn–(Al–Si) steels investigated by experiment and theory. *Acta Mater.* **2014**, *68*, 238–253. [CrossRef]
69. Kim, J.; Lee, S.J.; De Cooman, B.C. Effect of Al on the stacking fault energy of Fe–18Mn–0.6 C twinning-induced plasticity. *Scr. Mater.* **2011**, *65*, 363–366. [CrossRef]
70. Lee, Y.K.; Choi, C. Driving force for $\gamma \rightarrow \varepsilon$ martensitic transformation and stacking fault energy of $\gamma$ in Fe-Mn binary system. *Metall. Mater. Trans. A* **2000**, *31*, 355–360. [CrossRef]
71. Saeed-Akbari, A.; Imlau, J.; Prahl, U.; Bleck, W. Derivation and Variation in Composition-Dependent Stacking Fault Energy Maps Based on Subregular Solution Model in High-Manganese Steels. *Met. Mater. Trans. A* **2009**, *40*, 3076–3090. [CrossRef]
72. Grässel, O.; Frommeyer, G.; Derder, C.; Hofmann, H. Phase Transformations and Mechanical Properties of Fe-Mn-Si-Al TRIP-Steels. *J. Phys. Colloq.* **1997**, *07*, C5-383–C5-388. [CrossRef]
73. Jeong, J.; Woo, W.; Oh, K.; Kwon, S.; Koo, Y. In situ neutron diffraction study of the microstructure and tensile deformation behavior in Al-added high manganese austenitic steels. *Acta Mater.* **2012**, *60*, 2290–2299. [CrossRef]
74. Jin, J.-E.; Lee, Y.-K. Effects of Al on microstructure and tensile properties of C-bearing high Mn TWIP steel. *Acta Mater.* **2012**, *60*, 1680–1688. [CrossRef]
75. Jeong, K.; Jin, J.E.; Jung, Y.S.; Kang, S.; Lee, Y.K. The effects of Si on the mechanical twinning and strain hardening of Fe–18Mn–0.6 C twinning-induced plasticity steel. *Acta Mater.* **2013**, *61*, 3399–3410. [CrossRef]
76. Cabañas, N.; Penning, J.; Akdut, N.; De Cooman, B.C. High-temperature deformation properties of austenitic Fe-Mn alloys. *Met. Mater. Trans. A* **2006**, *37*, 3305–3315. [CrossRef]
77. Sastri, V.; Bünzli, J.-C.; Rao, V.R.; Rayudu, G.; Perumareddi, J. *Modern Aspects of Rare Earths and Their Complexes*; Elsevier: Amsterdam, The Netherlands, 2003. [CrossRef]
78. Kippenhan, N.; Gschneidner, K.A., Jr. *Rare-Earth Metals in Steels (No. IS-RIC-4)*; Iowa State University of Science and Technology, Rare-Earth Information Center: Ames, IA, USA, 1970.
79. Ji, Y.; Zhang, M.-X.; Ren, H. Roles of Lanthanum and Cerium in Grain Refinement of Steels during Solidification. *Metals* **2018**, *8*, 884. [CrossRef]
80. Kim, S.J.; Ryu, K.M.; Oh, M.-S. Addition of cerium and yttrium to ferritic steel weld metal to improve hydrogen trapping efficiency. *Int. J. Miner. Met. Mater.* **2017**, *24*, 415–422. [CrossRef]
81. Liu, Y.; Li, J.; Geng, R.; Zhi, J.; Lu, B. Effect of Cerium Content on Precipitation Behavior of Inclusions in High-Strength Low-Alloy Steel. *Met. Microstruct. Anal.* **2022**, *11*, 560–568. [CrossRef]
82. Adabavazeh, Z.; Hwang, W.S.; Su, Y.H. Effect of Adding Cerium on Microstructure and Morphology of Ce-Based Inclusions Formed in Low-Carbon Steel. *Sci. Rep.* **2017**, *7*, 46503. [CrossRef] [PubMed]
83. Li, G.; Lan, P.; Zhang, J.; Wu, G. Refinement of the Solidification Structure of Austenitic Fe-Mn-C-Al TWIP Steel. *Met. Mater. Trans. B* **2020**, *51*, 452–466. [CrossRef]

84. Daamen, M.; Richter, S.; Hirt, G. Microstructure Analysis of High-Manganese TWIP Steels Produced via Strip Casting. In *Key Engineering Materials*; Trans Tech Publications Ltd.: Bäch, Switzerland, 2013; Volume 554–557, pp. 553–561. [CrossRef]
85. Daamen, M.; Haase, C.; Dierdorf, J.; Molodov, D.A.; Hirt, G. Twin-roll strip casting: A competitive alternative for the production of high-manganese steels with advanced mechanical properties. *Mater. Sci. Eng. A* **2015**, *627*, 72–81. [CrossRef]
86. Rajinikanth, V.; Mukherjee, K.; Chowdhury, S.G.; Schiebahn, A.; Harms, A.; Bleck, W. Mechanical property and microstructure of resistance spot welded twinning induced plasticity-dual phase steels joint. *Sci. Technol. Weld. Join.* **2013**, *18*, 485–491. [CrossRef]
87. Lan, P.; Tang, H.; Zhang, J. Hot ductility of high alloy Fe–Mn–C austenite TWIP steel. *Mater. Sci. Eng. A* **2016**, *660*, 127–138. [CrossRef]
88. Wu, L.; Zhi, J.; Zhang, J.; Zhao, B.; Liu, Q. Effect of Cerium on the Microstructure and Inclusion Evolution of C-Mn Cryogenic Vessel Steels. *Materials* **2021**, *14*, 5262. [CrossRef]
89. Guo, Y.; Sun, S.; Song, S. Effect of minor rare earth cerium addition on the hot ductility of a reactor pressure vessel steel. *Results Phys.* **2019**, *15*, 102746. [CrossRef]
90. Guo, Y.; Zhao, Y.; Song, S. Highly Enhanced Hot Ductility Performance of Advanced SA508-4N RPV Steel by Trace Impurity Phosphorus and Rare Earth Cerium. *Metals* **2020**, *10*, 1598. [CrossRef]
91. Trang, T.; Lee, S.-Y.; Heo, Y.-U.; Kang, M.-H.; Lee, D.-H.; Lee, J.S.; Yim, C.H. Improved hot ductility of an as-cast high Mn TWIP steel by direct implementation of an MnS-containing master alloy. *Scr. Mater.* **2022**, *215*, 114685. [CrossRef]
92. Saeidi, N.; Raeissi, M. Promising effect of copper on the mechanical properties of transformation-induced plasticity steels. *Mater. Sci. Technol.* **2019**, *35*, 1708–1716. [CrossRef]
93. Traint, S.; Pichler, A.; Hauzenberger, K.; Stiaszny, P.; Werner, E. Influence of silicon, aluminium, phosphorus and copper on the phase transformations of low alloyed TRIP-steels. *Steel Res.* **2002**, *73*, 259–266. [CrossRef]
94. Kim, S.-J.; Gil Lee, C.; Lee, T.-H.; Oh, C.-S. Effects of Copper Addition on Mechanical Properties of 0.15C-1.5Mn-1.5Si TRIP-aided Multiphase Cold-rolled Steel Sheets. *ISIJ Int.* **2002**, *42*, 1452–1456. [CrossRef]
95. Kim, S.-J.; Gil Lee, C.; Lee, T.-H.; Oh, C.-S. Effect of Cu, Cr and Ni on mechanical properties of 0.15 wt.% C TRIP-aided cold rolled steels. *Scr. Mater.* **2003**, *48*, 539–544. [CrossRef]
96. Lee, S.; Kim, J.; Lee, S.J.; De Cooman, B.C. Effect of Cu addition on the mechanical behavior of austenitic twinning-induced plasticity steel. *Scr. Mater.* **2011**, *65*, 1073–1076. [CrossRef]
97. Jung, J.-G.; Jung, M.; Lee, S.-M.; Shin, E.; Shin, H.-C.; Lee, Y.-K. Cu precipitation kinetics during martensite tempering in a medium C steel. *J. Alloys Compd.* **2013**, *553*, 299–307. [CrossRef]
98. Skoufari-Themistou, L.; Crowther, D.; Mintz, B. Strength and impact behaviour of age hardenable copper containing steels. *Mater. Sci. Technol.* **1999**, *15*, 1069–1079. [CrossRef]
99. Han, K.; Yoo, J.; Lee, B.; Han, I.; Lee, C. Effect of Ni on the hot ductility and hot cracking susceptibility of high Mn austenitic cast steel. *Mater. Sci. Eng. A* **2014**, *618*, 295–304. [CrossRef]
100. Peng, X.; Zhu, D.; Hu, Z.; Yi, W.; Liu, H.; Wang, M. Stacking fault energy and tensile deformation behavior of high-carbon twinning-induced plasticity steels: Effect of Cu addition. *Mater. Des.* **2013**, *45*, 518–523. [CrossRef]
101. Comineli, O.; Qaban, A.; Mintz, B. Influence of Cu and Ni on the Hot Ductility of Low C Steels with Respect to the Straightening Operation When Continuous Casting. *Metals* **2022**, *12*, 1671. [CrossRef]
102. Holappa, L.; Wijk, O. Inclusion engineering. *Treatise Process Metall.* **2014**, 347–372.
103. Lehmann, J.; Meilland, R. Inclusion cleanness in calcium-treated steel grades. In *The SGTE Casebook*; Woodhead Publishing: Sawston, UK, 2008; pp. 267–272.
104. Theyssier, M.C. Manufacturing of advanced high-strength steels (AHSS). In *Welding and Joining of Advanced High Strength Steels (AHSS)*; Woodhead Publishing: Sawston, UK, 2015; pp. 29–53.
105. Baker, T.N. Role of zirconium in microalloyed steels: A review. *Mater. Sci. Technol.* **2014**, *31*, 265–294. [CrossRef]
106. Turkdogan, E.T. Causes and effects of nitride and carbonitride precipitation in HSLA steels in relation to continuous casting. In *Steelmaking Conference Proceedings*; AIME: New York, NY, USA, 1987; Volume 70, pp. 399–409.
107. Karjalainen, L.P.; Kinnunen, H.; Porter, D. Hot Ductility of Certain Microalloyed Steels under Simulated Continuous Casting Conditions. In *Materials Science Forum*; Trans Tech Publications Ltd.: Bäch, Switzerland, 1998; Volume 284–286, pp. 477–484. [CrossRef]
108. Coleman, T.H.; Wilcox, J.R. Transverse cracking in continuously cast HSLA slabs–influence of composition. *Mater. Sci. Technol.* **1985**, *1*, 80–83. [CrossRef]